Synthesis, Pharmacological Characterization and Docking Analysis of a Novel Family of Diarylisoxazoles as Highly Selective COX-1 Inhibitors.

ARTICLE *in* JOURNAL OF MEDICINAL CHEMISTRY · MAY 2013

Impact Factor: 5.45 · DOI: 10.1021/jm301905a · Source: PubMed

11 AUTHORS, INCLUDING:

Stefania Tacconelli
Università degli Studi G. d'Annunzio Chieti e P…
65 PUBLICATIONS **2,199** CITATIONS
SEE PROFILE

Antonio Scilimati
Università degli Studi di Bari Aldo Moro
79 PUBLICATIONS **925** CITATIONS
SEE PROFILE

Antonio Lavecchia
University of Naples Federico II
118 PUBLICATIONS **2,415** CITATIONS
SEE PROFILE

Melania Dovizio
Università degli Studi G. d'Annunzio Chieti e P…
26 PUBLICATIONS **348** CITATIONS
SEE PROFILE

Journal of Medicinal Chemistry

Article

pubs.acs.org/jmc

Synthesis, Pharmacological Characterization, and Docking Analysis of a Novel Family of Diarylisoxazoles as Highly Selective Cyclooxygenase-1 (COX-1) Inhibitors

Paola Vitale,[†,#] Stefania Tacconelli,[§,⊥,#] Maria Grazia Perrone,[†,#] Paola Malerba,[†] Laura Simone,[†] Antonio Scilimati,[*,†] Antonio Lavecchia,[*,‡] Melania Dovizio,[§,⊥] Emanuela Marcantoni,[§,⊥] Annalisa Bruno,[∥,⊥] and Paola Patrignani[*,§,⊥]

[†]Dipartimento di Farmacia-Scienze del Farmaco, Università degli Studi di Bari "A. Moro", Via Orabona 4, 70125 Bari, Italy

[‡]Dipartimento di Farmacia, "Drug Discovery" Laboratory, Università di Napoli "Federico II", Via D. Montesano 49, 80131 Napoli, Italy

[§]Department of Neuroscience and Imaging, [∥]Department of Medicine and Aging, "G. d'Annunzio" University, and [⊥]Center of Excellence on Aging (CeSI), Chieti, Italy

Supporting Information

ABSTRACT: 3-(5-Chlorofuran-2-yl)-5-methyl-4-phenylisoxazole (**P6**), a known selective cyclooxygenase-1 (COX-1) inhibitor, was used to design a new series of 3,4-diarylisoxazoles in order to improve its biochemical COX-1 selectivity and antiplatelet efficacy. Structure−activity relationships were studied using human whole blood assays for COX-1 and COX-2 inhibition in vitro, and results showed that the simultaneous presence of 5-methyl (or -CF_3), 4-phenyl, and 5-chloro(-bromo or -methyl)furan-2-yl groups on the isoxazole core was essential for their selectivity toward COX-1. **3g**, **3s**, **3d** were potent and selective COX-1 inhibitors that affected platelet aggregation in vitro through the inhibition of COX-1-dependent thromboxane (TX) A_2. Moreover, we characterized their kinetics of COX-1 inhibition. **3g**, **3s**, and **3d** were more potent inhibitors of platelet COX-1 and aggregation than **P6** (named **6**) for their tighter binding to the enzyme. The pharmacological results were supported by docking simulations. The oral administration of **3d** to mice translated into preferential inhibition of platelet-derived TXA_2 over protective vascular-derived prostacyclin (PGI_2).

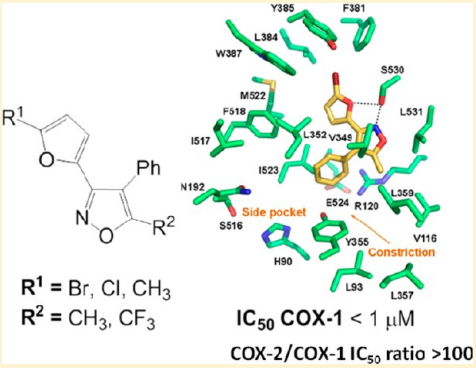

INTRODUCTION

Cyclooxygenase-1 (COX-1) and cyclooxygenase-2 (COX-2) catalyze the first step of the biosynthesis of prostanoids from arachidonic acid (AA).[1] Different from COX-2 gene that is mainly inducible, COX-1 is a housekeeping gene constitutively expressed in almost all mammalian tissues and cells.[1] However, the expression of COX-1 can be regulated in some circumstances, such as during development.[2] In physiological conditions, COX-1 is highly expressed in the gastrointestinal (GI) tract and platelets,[3,4] where it is involved in the generation of cytoprotective prostaglandin (PG)E_2 and platelet proaggregatory thromboxane (TX) A_2, respectively.[1]

COX-1 plays a role in several pathological conditions such as thrombosis, atherosclerosis, and tumorigenesis.[5−10] Importantly, platelet COX-1 is the target of one of the most efficacious antithrombotic agents used for prevention of vascular occlusive events, i.e., aspirin.[11]

Aspirin irreversibly acetylates Ser529 and Ser516 of COX-1 and COX-2, respectively,[12] leading to irreversible enzyme inactivation. Because of pharmacokinetics features (i.e., short half-life of 20 min) and pharmacodynamics features (higher potency to inhibit COX-1 than COX-2), low doses of aspirin (75−100 mg once daily) act by affecting platelet COX-1 activity while they cause only a marginal and transient inhibitory effect on COX-2 and extra-platelet cellular COX-1. Low doses of aspirin cause an almost complete suppression (≥95%) of platelet TXA_2 generation ex vivo, persisting throughout the dosing interval (i.e., 24 h).[11,13] This is a fundamental requisite to obtain an antiplatelet effect,[14] since even tiny concentrations of TXA_2 may activate platelets and importantly they synergize with other platelet agonists.[15] The antiplatelet effect of aspirin is strictly related to platelet turnover.[11,12] Thus, enhanced platelet turnover rate detected in some cardiovascular (CV) conditions, such as diabetes, might decrease the efficacy of the drug to halt almost completely platelet TXA_2 generation.[16] Moreover, we have recently shown that platelets contain COX-1 mRNA and the enzymatic machinery for protein synthesis; thus, these anucleated megacaryocyte fragments are able to synthesize de novo COX-1 in response to platelet activation in vitro.[17] Thus,

Received: December 28, 2012
Published: May 7, 2013

Table 1. Inhibitory Effect of 6 and Its Diarylisoxazole Derivatives on COX-1 and COX-2 Activity in Vitro in Human Whole Blood Assays[a]

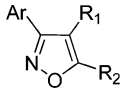

				IC$_{50}$ (μM)		
	Ar	R_1	R_2	COX-1	COX-2	COX-2/COX-1 IC$_{50}$ ratio
3a	3-chlorophenyl	C_6H_5	CH_3	1.30 (0.54−3.30)	0.27 (0.09−0.76)	0.21
3b	2-chlorophenyl	C_6H_5	CH_3	0.27 (0.13−0.58)	1.10 (0.40−3.20)	4.07
3d	5-chlorofuran-2-yl-	C_6H_5	CF_3	0.81 (0.52−1.24)	>100	>123.46
3e	5-chlorofuran-2-yl-	2-FC_6H_4	CH_3	1.90 (1.30−2.70)	>100	>52.63
3f	5-chlorofuran-2-yl-	4-FC_6H_4	CH_3	1.90 (0.80−4.70)	17.20 (4.00−63.00)	9.05
3g	5-methylfuran-2-yl-	C_6H_5	CH_3	0.32(0.24−0.42)	68.20 (41.00−114.50)	213.12
3h	5-chlorofuran-2-yl-	C_6H_5	CO_2H	>100	>100	
3i	5-chlorofuran-2-yl-	C_6H_5	CO_2CH_3	19.20 (8.30−44.50)	>100	>5.21
3l	5-chlorofuran-2-yl-	C_6H_5	CH_2OH	4.20 (2.90−6.40)	>100	>23.81
3m	5-chlorofuran-2-yl-	C_6H_5	CH_2OCOCH_3	5(2−12)	>100	>20
3n	5-chlorofuran-2-yl-	C_6H_5	$CO_2(CH_2)_3$-morpholine	>100	>100	
3p	5-chlorofuran-2-yl-	C_6H_5	$CO_2(CH_2)_3ONO_2$	>100	>100	
3q	furan-2-yl-	C_6H_5	CH_3	2.20 (1.00−4.00)	20.44 (8.00−52.00)	9.29
3r	tetrahydrofuran-2-yl-	C_6H_5	CH_3	>100	>100	
3s	5-bromofuran-2-yl-	C_6H_5	CH_3	0.33 (0.18−0.41)	34 (19−59)	103.03
3t	5-chlorofuran-2-yl-	CO_2CH_3	C_6H_5	17.40 (9.20−33.00)	>100	>5.75
3v	5-chlorofuran-2-yl-	CO_2H	C_6H_5	>100	>100	
3u	C_6H_5	CO_2CH_3	C_6H_5	17.28 (5.40−56.70)	>100	>5.79
3w	C_6H_5	CO_2H	C_6H_5	>100	>100	
4	5-chlorofuran-2-yl-	C_6H_5	CH_3	>100	>100	
5	furan-2-yl-	C_6H_5	CH_3	37 (13−106)	>100	>2.70
6	5-chlorofuran-2-yl-	C_6H_5	CH_3	0.50(0.26−0.92)	>100	>200

[a] IC$_{50}$ values are reported as the mean of at least three measurements. In the parentheses, IC$_{50}$ confidence intervals are reported.

we hypothesized that a reversible inhibitor of platelet COX-1 may be useful as antiplatelet agent in some patients with CV disease where low-dose aspirin failed to completely affect platelet TXA_2 generation.

Naproxen is a weak, time-dependent reversible inhibitor of platelet COX-1 and is the only traditional (t) nonsteroidal anti-inflammatory drug (NSAID) (also known as nonselective NSAID) that causes a profound and persistent COX-1 inhibition due to its long half-life when given at high doses.[18,19] This effect on platelet COX-1 is plausibly involved in a better CV safety profile of naproxen than other tNSAIDs.[20] However, naproxen use in the general population is not cardioprotective for two major reasons: (i) it is associated with variability in causing complete (>95%) suppression of the maximal capacity of platelets to generate TXA_2 at dosing interval (i.e., 12 h after dosing) which, however, can be reduced at high doses;[21,22] (ii) it can cause a profound reduction of the biosynthesis of vasoprotective prostacyclin (PGI_2) by inhibiting COX-2 activity in the vasculature.[19,22]

A selective inhibitor of COX-1 may be associated with improved CV safety compared with naproxen because in front of a profound suppression of platelet COX-1, it may leave PGI_2 to act by restraining (i) platelet activation induced by all platelet agonists, not only TXA_2, (ii) coagulation for its capacity to induce thrombomodulin, (iii) oxidative stress for its capacity to induce heme oxygenase-1.[23] Finally, PGI_2 may cause vasodilation and inhibition of vascular smooth muscle cells proliferation.[23]

Selective inhibitors of COX-1 may be associated with enhanced risk of upper GI bleeding (UGIB) due to the inhibition of COX-1-derived prostanoids which are involved in the constitutive defense mechanism operating in physiological conditions. However, they could be better tolerated than tNSAIDs. In fact, it has been shown that tNSAIDs, which cause a profound and coincident inhibition of both COX-1 and COX-2, are associated with higher risk of UGIB.[24] This is mechanistically plausible with results obtained in the mouse showing that inhibition of both COX-1 and COX-2 is required for the formation of gastric lesions.[25]

The development of reversible and highly selective COX-1 inhibitors could provide valuable tools for investigating the role of COX-1 in tumorigenesis.[26,27] Recent studies have shown that low-dose aspirin which targets almost selectively platelet COX-1 reduces long-term incidence and mortality due to colorectal cancer and other types of cancer.[28,29] The use of reversible, selective COX-1 inhibitors will help to unravel the possible contribution of extra-platelet sources of COX-1 in tumorigenesis.[30]

In a previous study, we found that 3-(5-chlorofuran-2-yl)-5-methyl-4-phenylisoxazole (**P6**) is a highly selective COX-1 inhibitor.[31] Structure−activity relationship (SAR) studies of a series of diarylpyrazoles analogues of **P6** (named **6**) allowed us also to clarify that isoxazole core ring and the presence of furanyl group are crucial determinants for high COX-1 selectivity.[32] In the present study, we synthesized in fair to good yield a new series of diarylisoxazoles (Table 1). We compared **6** and novel compounds for (i) the degree of COX-1 selectivity in human whole blood[33,34] and (ii) the inhibition of platelet aggregation and TXB_2 generation in platelet rich plasma (PRP) in response to arachidonic acid (AA) or collagen. Since COX-1 activity is regulated by substrate-dependent cooperative activation which

dx.doi.org/10.1021/jm301905a | J. Med. Chem. 2013, 56, 4277−4299

can influence the affinity of many cyclooxygenase inhibitors for COX-1,[35] we compared concentration−response curves for inhibition of COX-1 activity in isolated human platelets by **6** and the novel COX-1 inhibitors in the presence of low and high concentrations of AA (i.e., 0.50 and 10 μM, respectively). Moreover, we studied the reversibility of the inhibition of COX-1 and COX-2 in two cell lines that selectively express only COX-1 or COX-2, i.e., the THP-1 human monocytic leukemia cell line or the MDA-MB-231 breast cancer cell line, respectively. We present the results of docking simulations of diarylisoxazole inhibitors at the COX-1 active site to predict the molecular determinants of the interaction. Among the novel diarylisoxazole derivatives, **3d** was administered to mice to assess the inhibitory effect on the systemic biosynthesis of TXA_2 and vascular PGI_2.[36]

RESULTS AND DISCUSSION

Rational Design of Novel Diarylisoxazoles. 3-(5-Chlorofuran-2-yl)-5-methyl-4-phenylisoxazole (herein **6**) was used to design a set of novel diarylisoxazoles (Table 1). We projected chloro-substituted 3-arylisoxazoles as **3a** and **3b** to evaluate the effect of the C_3-substituent modification both on the potency of these compounds to inhibit COX-1 and COX-2 activities and on the extent of their COX-1 selectivity, assessed in human whole blood assays. Moreover, to verify the role of the chlorine atom and of the aromaticity of the furanyl group at C_3 isoxazole ring position, we prepared the compounds **3g**, **3q**, **3r**, and **3s**. In addition, we studied the effects of the modifications on the group at isoxazole C_5 by using **3h**, **3i**, **3l**, and **3m**. In particular, **3m** is the acetoxy derivative of **6**. The introduction of a CF_3 group in place of a methyl in **6** provided 3-(5-chlorofuran-2-yl)-4-phenyl-5-trifluoromethylisoxazole (**3d**), a more stable lipophilic compound and eventually more stable from a metabolic viewpoint because the CF_3 group in place of a methyl does not undergo any transformation as shown in in vitro experiments with celecoxib;[37] thus, **3d** should not have a metabolism similar to that of valdecoxib (and potentially that of **6**).[38] The introduction of a fluorine atom at ortho- and para-position of the aromatic ring bonded at isoxazole C_4 of **6** gave **3e** and **3f** synthesized to further improve **6** metabolic stability, the ortho- and para-position of the phenyl ring at isoxazole C_4 being susceptible to enzyme-mediated hydroxylation reaction. Similarly, (*Z*)-4-amino-4-(5-chlorofuran-2-yl)-3-phenylbut-3-en-2-one (**4**) and (*Z*)-4-amino-4-(furan-2-yl)-3-phenylbut-3-en-2-one (**5**) were prepared as "ring-opened" analogues and as potential metabolites of **6**, since it is known that reduction of the isoxazole ring yields the formation of an enamino ketone metabolite in phase I metabolic pathways of valdecoxib.[30] Moreover, compounds having the aryl groups positioned at C_3 and C_5 of the isoxazole ring (**3t**, **3u**, **3w**, and **3v**) and not at C_3/C_4, were designed to evaluate the effect of their greater distance on the COX-1 inhibitory activity with respect to **6**. **3n** and **3p** bearing a NO-releasing group (morpholine and nitrate) linked through a spacer to the isoxazole ring were also designed and synthesized.

Synthesis of Novel Diarylisoxazoles. We have previously found that a number of 3,4-diarylisoxazoles structurally related to the valdecoxib, a selective COX-2 inhibitor, could be prepared by a two-step methodology: (a) 1,3-dipolar cycloaddition of arylnitrile oxides to the lithium enolate of phenylacetone, obtained by metalation with LDA at 0 °C and (b) the dehydration−aromatization reaction under basic (or acid) conditions of the 3-aryl-5-hydroxy-5-methyl-4-phenyl-2-isoxazoline intermediates.[31] By using the same synthetic methodology, we synthesized the novel compounds **3a−g** in high yields by a one-pot procedure starting from arylnitrile oxides and the enolates of 3-aryl-2-propanones, easily obtained with sodium hydride or lithium diisopropylamide at 0 °C (Scheme 1 and Table 2).

Scheme 1[a]

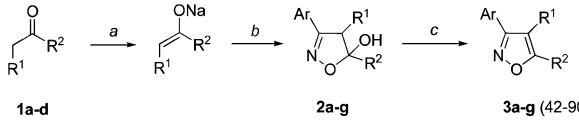

1a-d **2a-g** **3a-g** (42-90% yields)

[a]Reagents and conditions: (a) NaH/THF, 1 h, 0 °C; (b) ArCNO/THF, 12h, rt; aq NH_4Cl; (c) aq Na_2CO_3/MeOH.

We synthesized the 3-(5-chlorofuran-2-yl)-5-hydroxy-4-phenyl-4,5-dihydroisoxazole-5-carboxylic acid (**2h**) by 1,3-dipolar cycloaddition of 5-chlorofuran-2-yl nitrile oxide to the lithium dianion of phenylpyruvic acid obtained at 0 °C in the presence of LDA (2 equiv), followed by final treatment with HCl (Scheme 2).

However, the isolation through silica gel column chromatography of **2h** and its dehydration−aromatization reaction into the corresponding 3-(5-chlorofuran-2-yl)-4-phenylisoxazole-5-carboxylic acid (**3h**) under basic (or acid) conditions was unsuccessful. Thus, **2h** was first converted into its corresponding methyl ester **2i** in the presence of BF_3/MeOH, and after column chromatography over silica gel, **2i** was refluxed in MeOH and acqueous Na_2CO_3 to give **3h** in high yield (Scheme 2) (Ar = 5-chlorofuran-2-yl).

On the other hand, **3h** was also used as the starting material for the preparation of its methyl ester **3i**, as well as of the alcohol **3l**, in turn transformed into its acetoxymethyl derivative **3m** (Scheme 3).

Further, **3h** could also be converted into isoxazoles **3n−p** following the procedures depicted in Scheme 4.

3-(5-Chlorofuran-2-yl)-5-methyl-4-phenylisoxazole (**6**), obtained as previously reported,[24] was used as starting material for the preparation of **3q**, **3r**, **4**, and **5** by hydrogenation performed in the presence of a different catalyst (Scheme 5).

Isoxazole **3q** was transformed in high yield into **3s** by bromination in the presence of NBS/DMF (Scheme 6).

Differently, **3t** and **3u** (Ar = 5-chlorofuran-2-yl and Ar = phenyl, respectively) were synthesized in good yields by the 1,3-dipolar cycloaddition of the appropriate arylnitrile oxide to the methyl 3-phenylpropiolate in anhydrous CH_2Cl_2 (Scheme 7). From them, the corresponding carboxylic acid derivatives **3v** and **3w** were then quantitatively obtained by hydrolysis under basic conditions (KOH in THF).

Screening Strategy To Identify and Characterize Novel Highly Selective COX-1 Inhibitors. The extent of selectivity toward COX-1 by the novel diarylisoxazoles was assessed in human whole blood, in vitro,[33,34] by calculating COX-2/COX-1 IC_{50} ratios (Table 1 and Supporting Information Figure S1). In the first phase of the screening, COX-1 and COX-2 inhibition by the compounds was evaluated up to 100 μM (Table 1).

We selected three compounds (**3g**, **3s**, and **3d**) with IC_{50} values for COX-1 of <1 μM and high COX-1 selectivity (i.e., COX-2/COX-1 IC_{50} ratio of ≥100) and the acetoxy derivative of **6** (**3m**) (which might be able to acetylate COX-1 similarly to aspirin) for in-depth characterization of COX-1 selectivity and type of inhibitory mechanism of COX isozymes. In order to be able to define the degree of COX-1 selectivity in human whole

dx.doi.org/10.1021/jm301905a | J. Med. Chem. 2013, 56, 4277−4299

Table 2. Yields of 3,4-Diaryl-5-hydroxy-5-methyl-2-isoxazolines 2a−g and 3,4-Diaryl-5-methylisoxazoles 3a−g Obtained by 1,3-Dipolar Cycloaddition of Arylnitrile Oxides to Sodium Enolates of 3-Aryl-2-propanones 1a−d and Subsequent Dehydration−Aromatization under Basic Conditions[a]

Ar	R_1	R_2	yield (%) of **2a−g**	yield (%) of **3a−g**
3-chlorophenyl-	phenyl	CH_3	71 (**2a**)	71 (**3a**)
2-chlorophenyl-	phenyl	CH_3		78 (**3b**)
2-chlorophenyl-	2-fluorophenyl	CH_3		69 (**3c**)
5-chlorofuran-2-yl-	phenyl	CF_3	71 (**2d**)	65 (**3d**)
5-chlorofuran-2-yl-	2-fluorophenyl	CH_3	56 (**2e**)[b]	90 (**3e**)
5-chlorofuran-2-yl-	4-fluorophenyl	CH_3	62 (**2f**)[b]	62 (**3f**)
5-chlorofuran-2-yl-	phenyl	CH_3		70 (**6**)
5-methylfuran-2-yl-	phenyl	CH_3	23 (**2g**)[b]	42 (**3g**)

[a]Yields refer to the recrystallized products. [b]The apparent low yields are due to a spontaneous dehydration to isoxazoles.

Scheme 2[a]

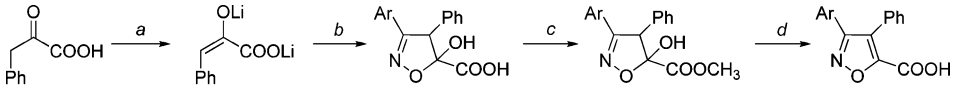

[a]Reagents and conditions: (a) 2 equiv of LDA, THF, 1 h, 0 °C; (b) ArCNO/THF, 16 h; sat. NH_4Cl; 2 N HCl; (c) BF_3/MeOH, rt, 3 h; (d) aq Na_2CO_3, MeOH, reflux.

Scheme 3[a]

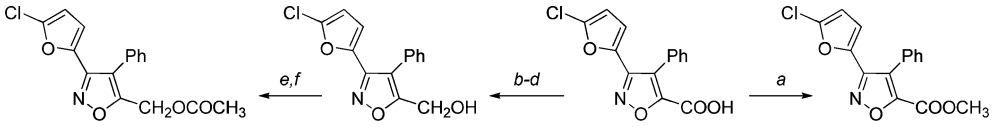

[a]Reagents and conditions: (a) H_2SO_4, MeOH, rt; (b) BMS, 5 h, rt; (c) H_2O; (d) 3 N NaOH and H_2O_2 (30%), 0.5 h; (e) Ac_2O/Et_3N, 0 °C to rt; (f) ice/$NaHCO_3$.

Scheme 4[a]

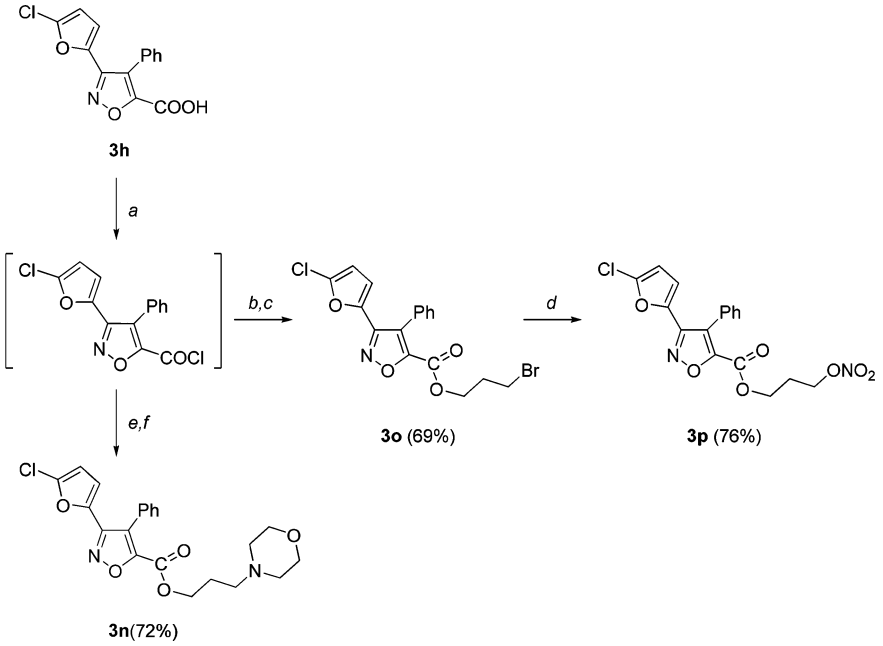

[a]Reagents and conditions: (a) $SOCl_2$, 2 h, reflux; (b) $Br(CH_2)_3OH/Et_3N$, CH_2Cl_2, 12 h; (c) aq Na_2CO_3; (d) $AgNO_3/CH_3CN$, 12 h; (e) 3-morpholinopropan-1-ol/Et_3N, CH_2Cl_2, 12 h, rt; (f) aq Na_2CO_3.

dx.doi.org/10.1021/jm301905a | J. Med. Chem. 2013, 56, 4277−4299

Scheme 5[a]

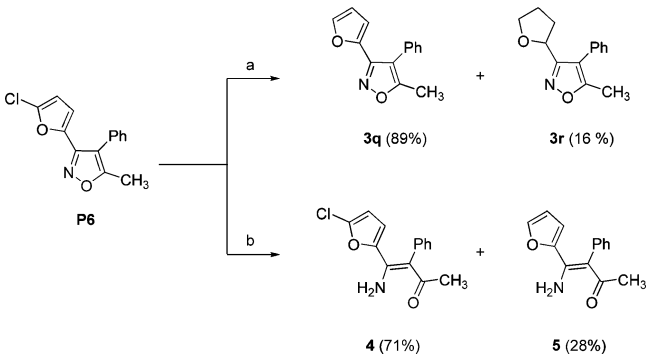

[a]Reagents and conditions: (a) H_2 (1 atm)/EtOH, PtO_2; (b) H_2 (1 atm)/EtOH, Raney Ni.

Scheme 6[a]

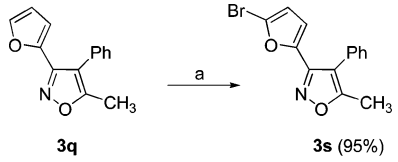

[a]Reagents and conditions: (a) 1.2 equiv of NBS/DMF, 0 °C.

Scheme 7[a]

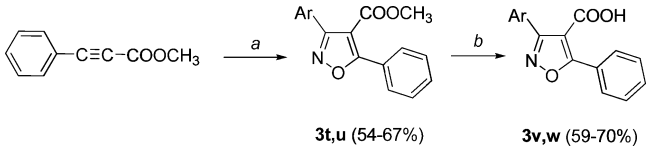

[a]Reagents and conditions: (a) ArCNO/CH_2Cl_2, 12 h, rt; (b) KOH/THF, 16 h, rt.

blood of the selected compounds, the concentration–response curves for inhibition of whole blood COX-2 were assessed up to 1000 μM. Moreover, they were assessed for (i) inhibition of platelet aggregation in PRP induced by AA or collagen and (ii) inhibition of TXB_2 generation in AA- or collagen-stimulated PRP. Moreover, we evaluated the concentration–response curves for inhibition of platelet COX-1 activity by **3s**, **6**, and **3m** in human washed platelets in the presence of low and high concentrations of AA (0.50 and 10 μM, respectively). Reversibility of the inhibition of COX-1 and COX-2 was studied in two cell lines that selectively expressed only COX-1 or COX-2, i.e., the THP-1 human monocytic leukemia cell line or the MDA-MB-231 breast cancer cell line, respectively. In all these experiments, **6** was used as reference compound.

Inhibitory Effects of the Diarylisoxazole Derivatives on COX-1 and COX-2 Activities in Human Whole Blood. In human whole blood, allowed to clot at 37 °C for 1 h, we detected 452 ± 32 ng/mL TXB_2 (mean ± SEM, n = 28), which is generated by platelet COX-1 activity.[34] Fourteen out of 21 compounds inhibited platelet COX-1 activity in a concentration-dependent fashion (Figure S1), and the IC_{50} values were reported in Table 1. In contrast, seven compounds did not affect platelet COX-1 activity up to 100 μM (Table 1). All compounds were assessed for the capacity to inhibit LPS-induced COX-2 activity in whole blood, and the IC_{50} values were reported in Table 1. Fifteen compounds, assessed up to 100 μM, inhibited COX-2 activity less than 50%. We selected three compounds showing both an IC_{50} for COX-1of <1 μM and a COX-2/COX-1 selectivity of ≥100 (i.e., **3s**, **3g**, and **3d**).

3s and **3g** showed IC_{50} values for COX-1 that were approximately 2-fold lower than that of **6**. **3d** showed an IC_{50} value for COX-1 comparable to that of **6** (Table 1). In order to define the IC_{50} values for inhibition of COX-2 by these three compounds and **6**, concentration–response curves were performed at concentrations up to 1000 μM (Figure 1A–D). At 1000 μM, **6** inhibited COX-2 activity by 61.00 ± 5.20% which was not statistically different from that caused by **3d** (49 ± 3%). Altogether our data showed that **6** and **3d** had similar potency to inhibit COX-1 and COX-2 in whole blood and had a comparable COX-1 selectivity of >1000 (Table 1 and Figure 1A and Figure 1D, respectively). Differently, **3s** and **3g** inhibited COX-2 activity with the following IC_{50} values [expressed as mean and 95% confidence interval (CI)]: 34 (19–59) and 68.20 (41.00–114.50) μM, respectively (Table 1 and Figure 1B and Figure 1C) and showed lower COX-1 selectivity than **6** (Table 1 and Figure 1B and Figure 1C) (COX-2/COX-1 IC_{50} ratios: 103.03 and 213.12, respectively). Thus, **3s** and **3g** were more potent toward COX-1 than **6** and they were characterized by high COX-1 selectivity which however was lower than that shown by **6**.

The acetoxy derivative of **6** (i.e., **3m**) inhibited platelet COX-1 activity with an IC_{50} of 5 (2–12) μM (Figure 1E and Table 1) that was significantly higher (8-fold) than the value obtained by **6**. At 1000 μM, **3m** inhibited COX-2 activity by 40 ± 4%, and this value was lower than that caused by **6**. Thus, **3m** was less potent than **6** to inhibit both COX-isozymes in human whole blood.

In order to verify whether different IC_{50} values for inhibition of COX-1 and COX-2 by these novel compounds and **6** were driven by differences in binding to plasma proteins, we evaluated the degree of binding to human serum albumin (HSA) and α_1-acid glycoprotein (AGP) of **3d**, **3g**, **3s**, and **6**. The compounds showed high degree of protein binding (i.e., 94.30 ± 0.86, 94.70 ± 9.33, 96.10 ± 1.27, and 95.70 ± 0.49%, respectively, mean ± SEM, n = 6), and the values were not significantly different from each other.

Effects of Selected Compounds (3s, 3g, 3d, and 3m) and 6 on Platelet Aggregation and TXB_2 Generation in PRP. Compounds **3s**, **3g**, **3d**, and **3m** were assessed for their inhibitory effects on platelet aggregation induced by AA, 1 mM (Figure 2A,C,E,G) in comparison to **6** (Figure 3A). Up to 3 μM, **3s**, **3g**, and **3d** did not inhibit AA-induced platelet aggregation. In contrast, at 10 μM, they almost completely inhibited AA-induced platelet aggregation (96.33 ± 1.80%, 97.80 ± 1.60%, and 99.20 ± 0.60%, respectively) in a statistically significant fashion (P < 0.001 versus DMSO vehicle) (Figure 2A,C,E).

The three novel diarylisoxazole derivatives were more potent than **6** in inhibiting AA-induced platelet aggregation (Figure 2A,C,E and Figure 3A). In fact, **6** did not affect AA-induced platelet aggregation at 10 μM, but it required a concentration of 30 μM to almost completely abrogate the platelet response (97.00 ± 1.80%, P < 0.001 versus DMSO vehicle) (Figure 3A). Similar to **6**, **3m** significantly inhibited platelet response at 30 μM (97.00 ± 1.50%, P < 0.001 versus DMSO vehicle) (Figure 2G).

As shown in Figure 4A,C,E, **3s**, **3g**, and **3d** caused a concentration-dependent inhibition of collagen-induced platelet aggregation. Similar to AA-induced platelet aggregation, up to 3 μM, **3s**, **3g**, and **3d** did not significantly inhibit collagen-induced platelet aggregation. A profound and statistically significant (P < 0.001 versus DMSO vehicle) inhibition of collagen-induced platelet aggregation occurred at 10 μM (78.00 ± 7.50%, 66 ±

dx.doi.org/10.1021/jm301905a | J. Med. Chem. 2013, 56, 4277–4299

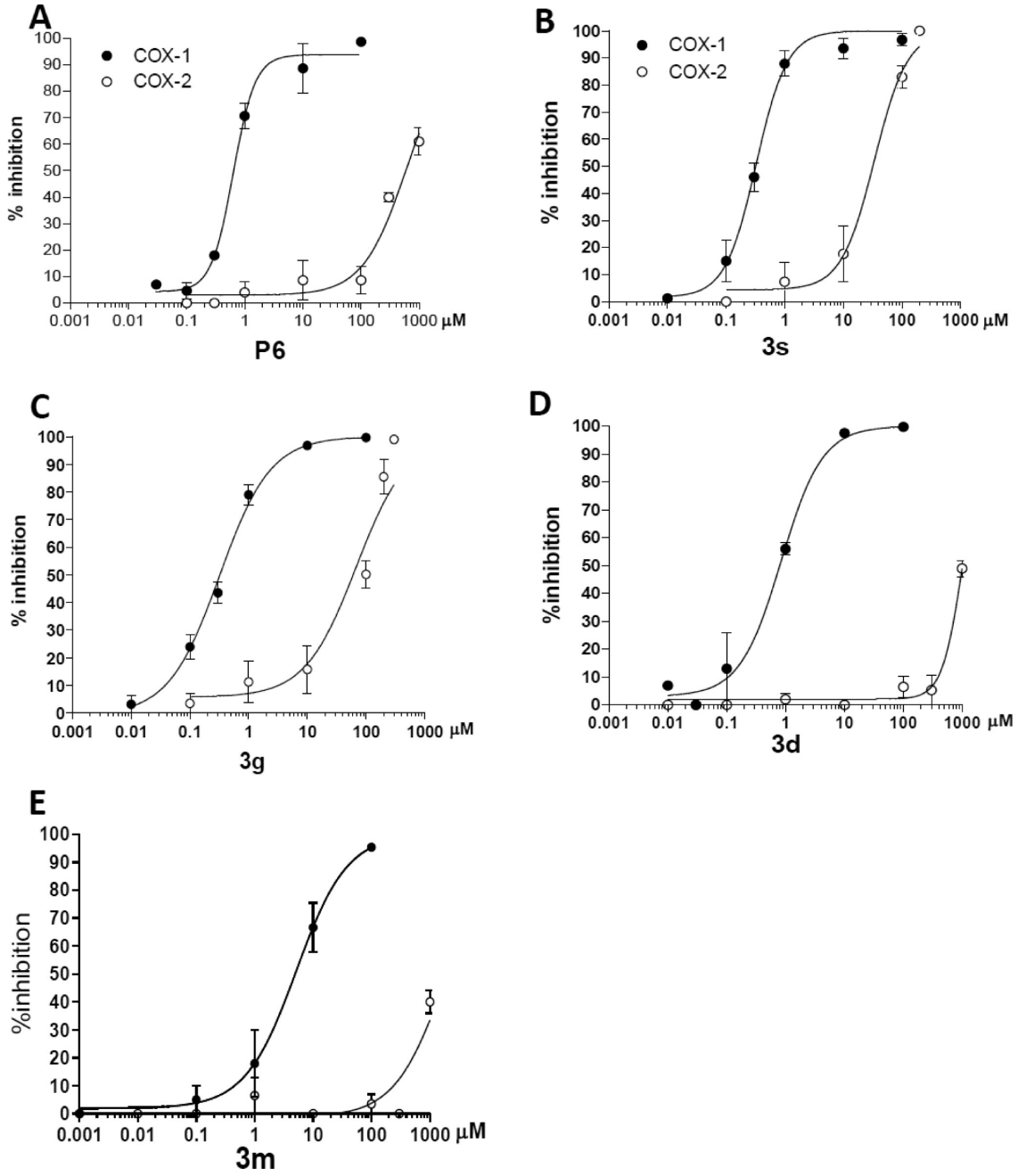

Figure 1. Concentration−response curves for the inhibition of whole blood COX-1 and COX-2 activities by **6** (A), **3s** (B), **3g** (C), **3d** (D), and **3m** (E). Increasing concentrations of **6** (0.10−1000 μM), **3s** (0.10−200 μM), **3g** (0.10−300 μM), **3d** (0.01−1000 μM), and **3m** (0.01−1000 μM) were incubated with 1 mL of heparinized whole blood samples, drawn from healthy volunteers (who had taken 300 mg of aspirin 48 h before sampling), in the presence of LPS (10 μg/mL) for 24 h, and plasma PGE_2 levels were assayed as a reflection of monocyte COX-2 activity (○). **6** (0.03−100 μM), **3s** (0.01−100 μM), **3g** (0.01−100 μM), **3d** (0.01−100 μM), and **3m** (0.001−100 μM) were also incubated with 1 mL of whole blood samples (drawn from healthy subjects when they had not taken any NSAID during the 2 weeks preceding the study) allowed to clot for 1 h, and serum TXB_2 levels were measured as a reflection of platelet COX-1 activity (●). Results are depicted as percentage inhibition, mean ± SEM, from three to nine separate experiments,.

12%, and 72 ± 9%, respectively). Even in collagen-induced platelet aggregation, **6** and **3m** required a concentration of 30 μM to cause a statistically significant inhibition of >50% (64.60 ± 5.00% and 62 ± 8%, $P < 0.01$ and $P < 0.001$ versus DMSO vehicle, respectively) (Figure 3C and Figure 4G).

Thus, although the novel diarylisoxazole derivatives showed a similar (**3d**) or a small higher potency (**3s** and **3g**) than **6** to inhibit platelet COX-1 activity in whole blood, they were all more potent than **6** to affect platelet aggregation in PRP induced by AA and collagen.

To clarify the reason for these results, we assessed TXB_2 generation in AA- and collagen-induced PRP before and after treatment with the different compounds. In PRP stimulated for 5 min with AA, 1 mM, we detected 1163 ± 220 ng/mL TXB_2 (n = 13). Compounds **3s**, **3g**, and **3d** inhibited TXB_2 generation in AA-stimulated PRP in a concentration-dependent fashion (Figure 2B,D,F) with comparable IC_{50} values of 3.40 (2.20−

dx.doi.org/10.1021/jm301905a | J. Med. Chem. 2013, 56, 4277−4299

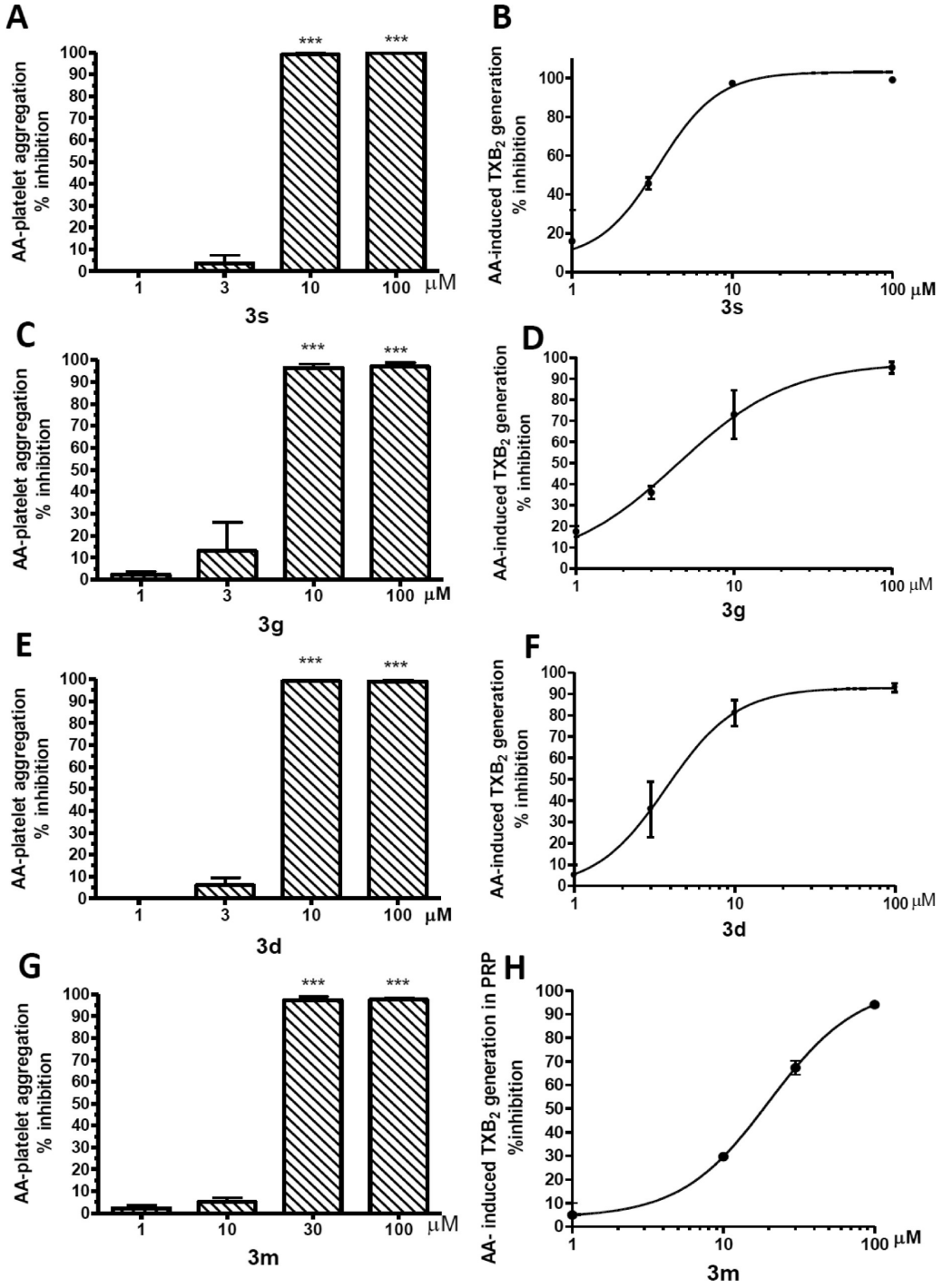

Figure 2. Effects of different concentrations of **3s** (A, B), **3g** (C, D), **3d** (E, F), and **3m** (G, H) on AA-induced platelet aggregation and TXB_2 generation in PRP. An amount of 1 μL of compounds (dissolved in DMSO) or vehicle was preincubated with platelet rich plasma (PRP) at 37 °C for 5 min at a final concentrations of 1−100 μM as shown in the different panels. Then PRP was stimulated by AA (1 mM) and platelet aggregation was followed up to 5 min using a Chrono-Log platelet aggregometer. TXB_2 levels in PRP were measured in AA-stimulated PRP after its incubation with **3s** (B), **3g** (D), **3d** (F), and **3m** (H). Results are depicted as the mean ± SEM of percentage of inhibition from three to five separate experiments: (***) $P < 0.001$ versus control.

5.30), 4.30 (2.00−10.00), 3.70 (2.00−7.00) μM, respectively, which were approximately 3-fold lower than the IC_{50} value of **6** [12 (7−20) μM] (Figure 3B). However, only the IC_{50} values of **3s** and **3d** were significantly different from that of **6**.

In PRP stimulated for 5 min with collagen, 2 μg/mL, we detected 82 ± 20 ng/mL TXB_2 ($n = 13$). As shown in parts B, D, and F of Figure 4, **3s**, **3g**, and **3d** inhibited TXB_2 generation in collagen-stimulated PRP in a concentration dependent fashion with comparable IC_{50} values of 7.60 (6.60−9.60), 7.40 (4.50−12.00), and 10 (9−11) μM, respectively. These values were lower than the **6** IC_{50} value [18.60 (11.00−32.00)μM] (Figure 3D), but a statistically significant difference was detected only for **3s** and **3d** versus **6**.

Differently, **3m** (Figure 2H and Figure 4H) inhibited TXB_2 generation in AA- and collagen-stimulated PRP with IC_{50} values of 20 (15−26) and 23.00 (13.00−42.50) μM, respectively, which

dx.doi.org/10.1021/jm301905a | J. Med. Chem. 2013, 56, 4277−4299

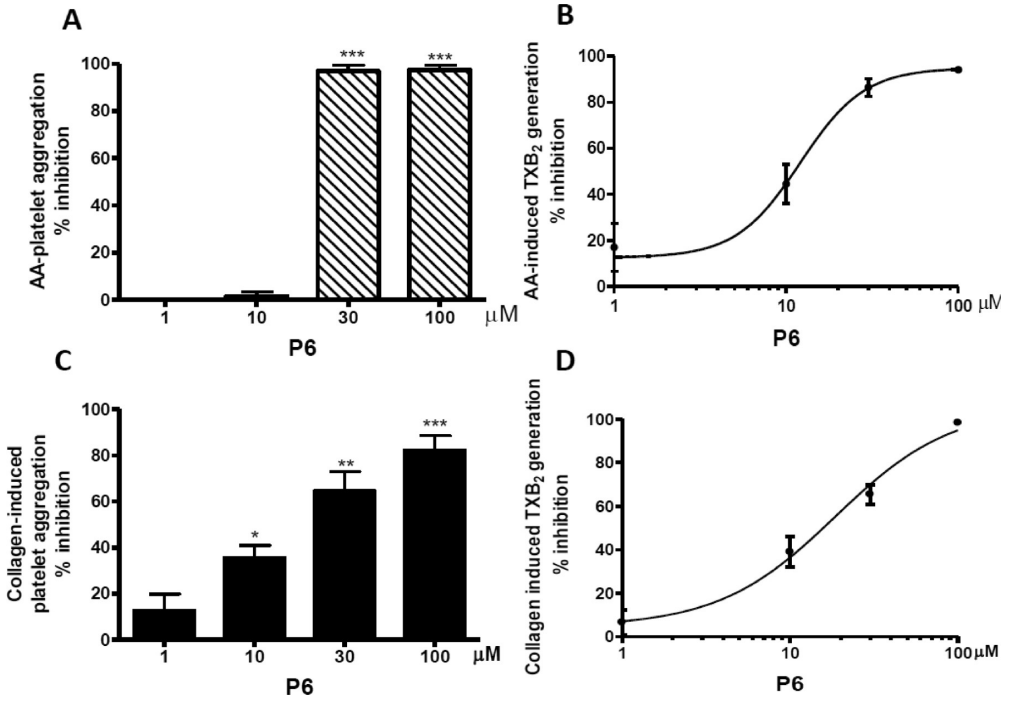

Figure 3. Effects of different concentrations of **6** on platelet aggregation and TXB_2 generation induced by AA (A, B) or induced by collagen (C, D). An amount of 1 μL of **6** (or vehicle) was preincubated with platelet rich plasma (PRP) at 37 °C for 5 min at a final concentrations of 1−100 μM. Then platelets were stimulated by AA (1 mM) (A) or by collagen (C) and platelet aggregation was measured in PRP using a Chrono-Log platelet aggregometer. TXB_2 levels in PRP were measured in AA-stimulated PRP (B) or in collagen-stimulated PRP (D) after its incubation with **6**. Results are depicted as the mean ± SEM of percentage of inhibition from three separate experiments: (***) $P < 0.001$, (**) $P < 0.01$, (*) $P < 0.05$ versus control.

were similar to that of **6** and significantly higher than those of **3s**, **3g**, and **3d**.

These results showed that all compounds inhibited TXB_2 generation in AA-stimulated PRP and collagen-stimulated PRP. However, we found that all compounds were less potent in inhibiting TXB_2 generation in PRP in response to AA, 1 mM, and collagen, 2 μg/mL, than in whole blood. Among the diarylisoxazole derivatives that we studied, **6** was the compound that has lost more potency to inhibit COX-1 in PRP versus whole blood.

Comparison of Concentration−Response Curves for Inhibition of Platelet COX-1 by Diarylisoxazole Derivative Compounds in the Presence of Low and High Concentrations of AA. Mechanistically, COX inhibitors fall into two broad categories: time-dependent/slowly reversible, such as indomethacin, and time-independent/rapidly reversible, such as ibuprofen.[39−41] Moreover, aspirin causes an irreversible inhibition of COX isozymes. To verify the type of mechanism of COX-1 inhibition by the novel diarylisoxazole derivatives and **6**, we performed experiments in washed human platelets and increasing concentrations of different compounds were preincubated with the cells to allow the possible formation of tightly bound enzyme−inhibitor complexes. Then AA, at low (0.50 μM) and high concentrations (10 μM), was added to initiate the reaction that was terminated after 30 min of incubation. We hypothesized that a rapidly reversible inhibitor, but not a slowly reversible inhibitor, should be characterized by a right shift of the log concentration−response curve for inhibition of TXB_2 obtained in the presence of high concentration of AA versus that obtained in the presence of low concentration of AA.

Human washed platelets pretreated with vehicle and then incubated with AA, 0.50 μM, for an additional 30 min at 37 °C generated 54.00 ± 7.90 ng/mL TXB_2 (n = 11). The production of TXB_2 by human washed platelets was significantly (P = 0.008) higher in the presence of 10 μM AA (680.00 ± 207.50 ng/mL, n = 10).

First, we studied the inhibitory effects of ibuprofen, aspirin, and indomethacin (Figure 5A−C). At 10 μM AA, ibuprofen caused a concentration-dependent reduction of TXB_2 generation with an IC_{50} value that was significantly higher than that found at 0.50 μM AA [1.86 (0.88−3.90) versus 0.29 (0.17−0.48)μM, respectively] (Figure 5A). In contrast, the concentration−response curves for inhibition of platelet COX-1 by indomethacin were not influenced by the concentration of AA (Figure 5B). Aspirin, which is an irreversible inhibitor of COX-1, inhibited platelet TXB_2 generation with comparable potency at the two different concentrations of AA used to initiate the enzymatic reaction (Figure 5C). Once we had the demonstration that the use of this experimental model is appropriate to discriminate between freely reversible and slowly reversible/irreversible inhibitors of COX-1, we tested the behavior of **3s**, **3g**, **3d**, **6**, and the acetoxy derivative of **6** (**3m**).

As shown in Figure 5D−F, **3s**, **3g**, and **3d** inhibited TXB_2 production in human washed platelets with similar IC_{50} values at both AA concentrations, which may suggest a strong interaction of the drug with platelet COX-1, similar to indomethacin. In contrast, in the presence of high concentrations of AA, the concentration−response curves for inhibition of platelet COX-1 activity by **6** and **3m** were right shifted compared to those obtained in the presence of low concentrations of AA (Figure 5G,H). This finding may suggest a weaker interaction of the two compounds with COX-1 than **3s**, **3g**, and **3d**.

Assessment of Reversibility of THP-1 Cell COX-1 Inhibition by Diarylisoxazole Derivatives. As shown in Figure 6A, THP-1 cells, cultured in suspension, constitutively expressed COX-1 but not COX-2. THP-1 cells incubated with

dx.doi.org/10.1021/jm301905a | J. Med. Chem. 2013, 56, 4277−4299

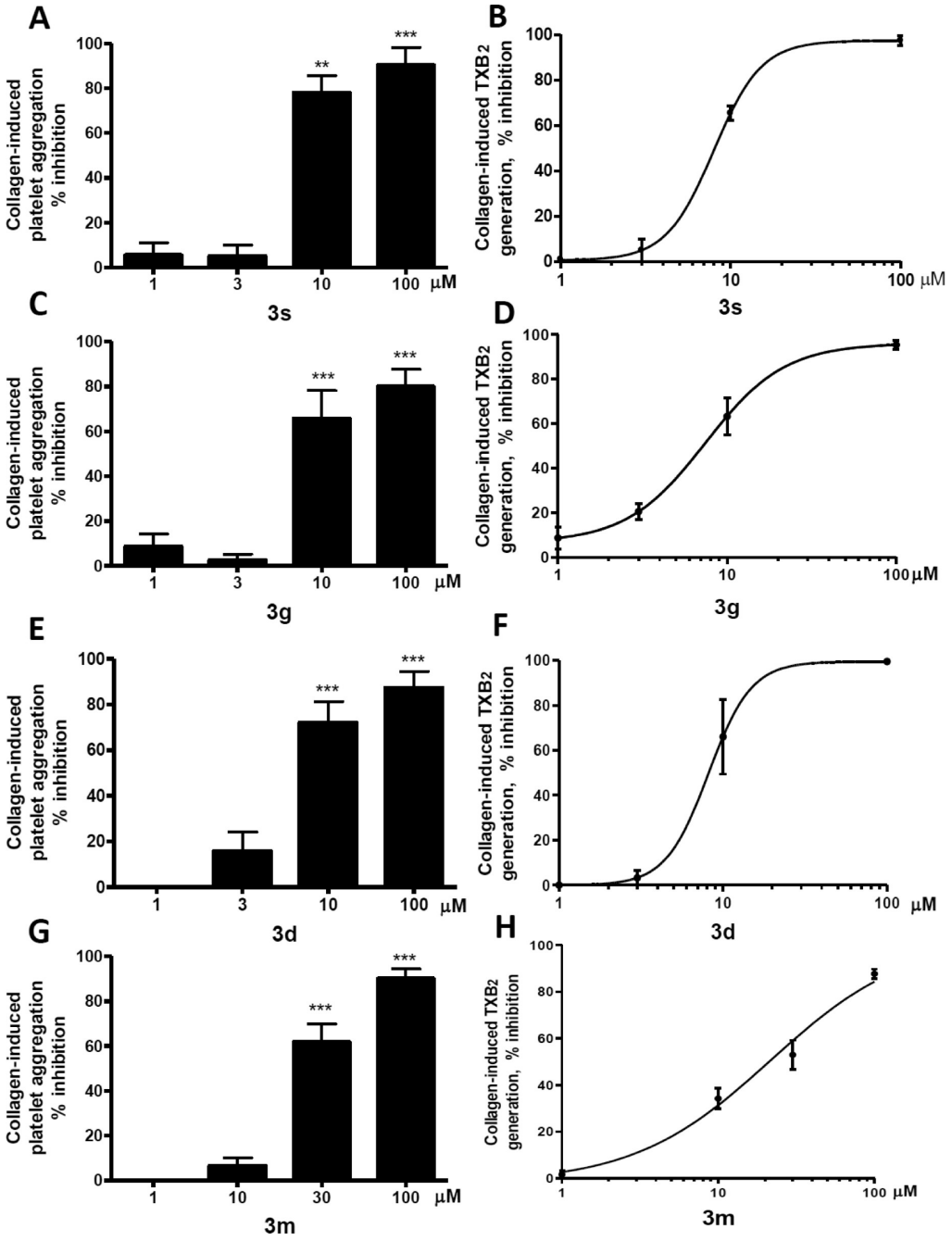

Figure 4. Effects of different concentrations of **3s** (A, B), **3g** (C, D), **3d** (E, F), and **3m** (G, H) on collagen-induced platelet aggregation and TXB_2 generation in PRP. An amount of 1 μL of compounds (dissolved in DMSO) or vehicle was preincubated with PRP at 37 °C for 5 min at a final concentrations of 1−100 μM as shown in the different panels. Then platelets were stimulated with collagen (2 μg/mL) and platelet aggregation was measured up to 5 min in PRP using a Chrono-Log platelet aggregometer. TXB_2 levels in PRP were measured in collagen-stimulated PRP after its incubation with **3s** (B), **3g** (D), **3d** (F), and **3m** (H). Results are depicted as the mean ± SEM of percentage of inhibition from three to five separate experiments: (***) $P < 0.001$, (**) $P < 0.01$ versus control.

vehicle (DMSO) for 30 min (at room temperature) and then stimulated with AA, 20 μM, for further 30 min (at 37 °C) generated TXB_2 (0.34 ± 0.05 pg/μg protein). At 100 μM **6**, four selected diarylisoxazole derivatives (**3s**, **3g**, **3d**, and **3m**), aspirin, indomethacin, and ibuprofen profoundly (≥90%) inhibited COX-1 activity ($P < 0.0001$ versus DMSO) (Figure 6B).

The profound inhibitory effect of COX-1 activity by aspirin, indomethacin, **3s**, **3g**, and **3d** persisted after extensive washing of cells (Figure 6B). This is consistent with the irreversible inhibition of COX-1 by aspirin and slow reversibility of the inhibition of COX-1 by indomethacin and the diarylisoxazole derivatives **3s**, **3g**, and **3d**. Differently, the profound inhibitory effect of COX-1 by ibuprofen was completely reverted by cell washing (Figure 6B), consistent with its mechanism of action of COX-1 inhibition which is rapidly reversible. The inhibition of COX-1 by **3m** and **6** was partially reversed (Figure 6B) by cell washing.

Altogether these results suggest that (i) similar to indomethacin, **3s**, **3g**, and **3d** had a strong interaction with COX-1 that is slowly reversible and (ii) the inhibition of COX-1

dx.doi.org/10.1021/jm301905a | J. Med. Chem. 2013, 56, 4277−4299

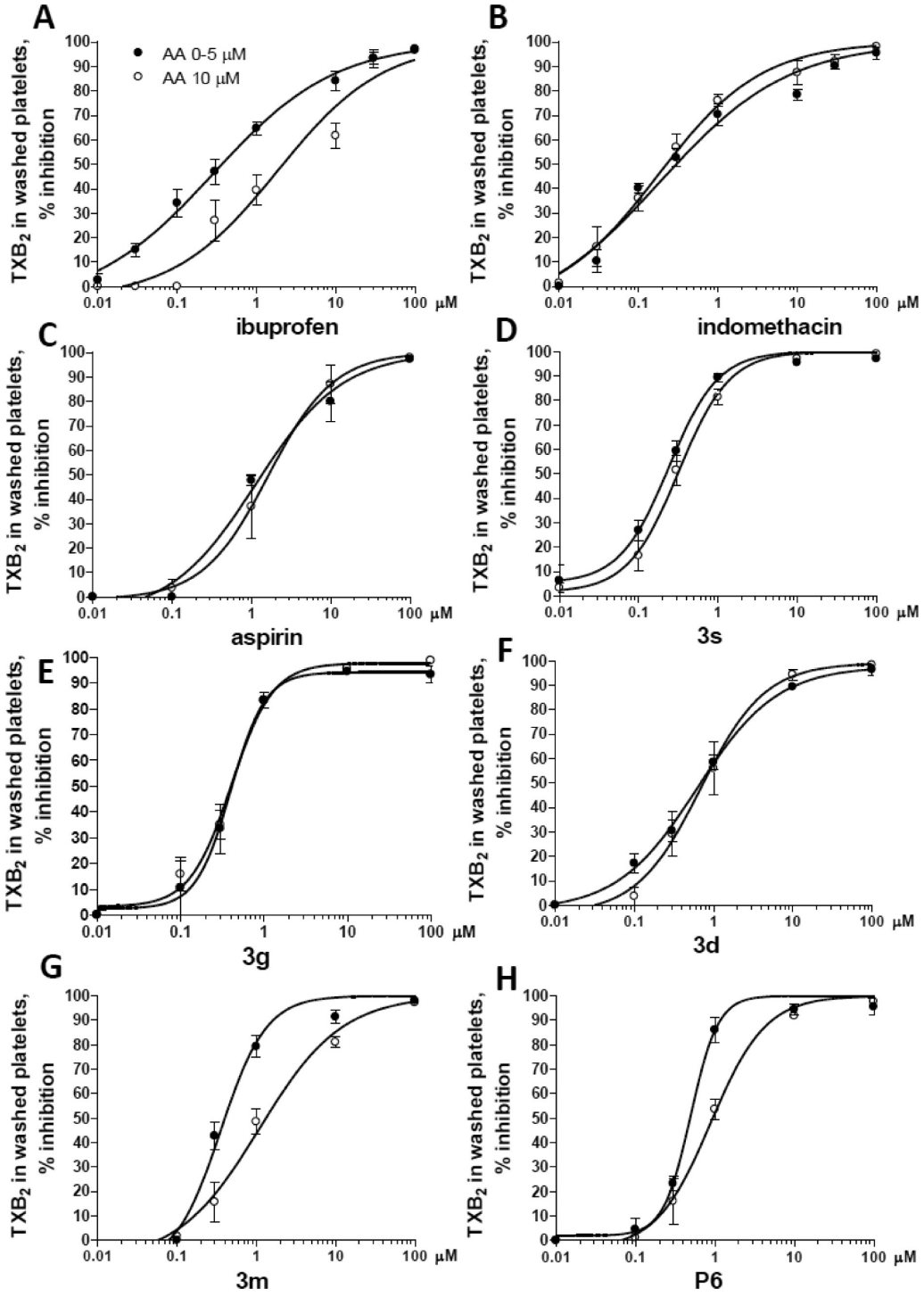

Figure 5. Concentration−response curves for the inhibition of TXB_2 production by human washed platelets by ibuprofen (A), indomethacin (B), aspirin (C), **3s** (D), **3g** (E), **3d** (F), **3m** (G), and **6** (H). Washed platelets (200 μL at a concentration of 10^8 cells/mL in HHBSS/10% anticoagulant) were incubated with increasing concentrations of different inhibitors (diluted from 400-fold concentrated solutions in DMSO or for aspirin in 95% HBSS 5% DMSO) for 25 min at 37 °C, and then 0.50 μM (●) or 10 μM (○) of AA was added for an additional 30 min at 37 °C. After centrifugation (760*g* for 10 min at 4 °C), TXB_2 levels were measured in the supernatant by specific RIA. Results are depicted as percentage inhibition, mean ± SEM, from three to six separate experiments.

by **3m** and **6** was reversible even if it occurred with a slower kinetics than that shown by ibuprofen (Figure 6B).

Assessment of Reversibility of MDA-MB231 Cell COX-2 Inhibition by Diarylisoxazole Derivatives. The reversibility of the interaction of the selected diarylisoxazole derivatives (**3s**, **3g**, **3d**, **3m**) and **6** with COX-2 was assessed in MDA-MB231 cells that expressed COX-2 but not COX-1 (Figure 7A). The effects of the novel compounds were compared with those of aspirin, indomethacin, and ibuprofen. Cells, preincubated with DMSO vehicle and then for further 30 min with AA, 0.50 μM, generated 1.40 ± 0.08 pg/μg proteins of PGE_2.

dx.doi.org/10.1021/jm301905a | J. Med. Chem. 2013, 56, 4277−4299

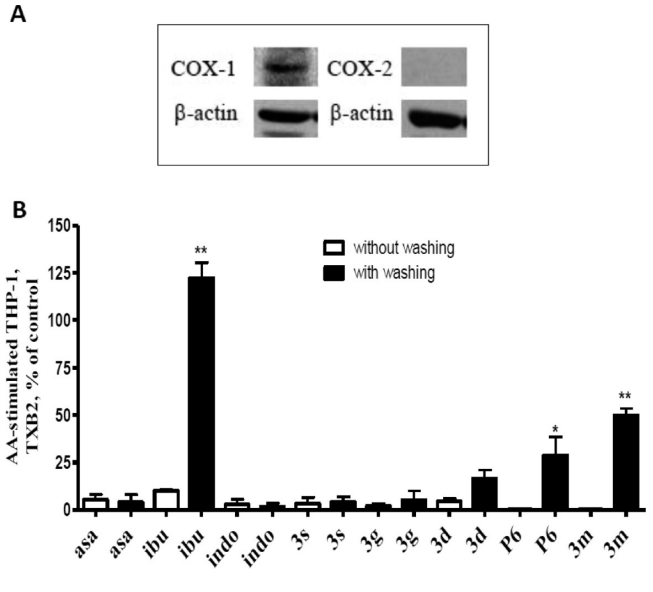

Figure 6. Assessment of COX-1 inhibition and its reversibility by diarylisoxazole derivatives in THP-1 cells Western blot analysis showed that THP-1 cells expressed only COX-1 but not COX-2 (A). These cells were preincubated with vehicle (DMSO) or with different compounds at a final concentration of 100 μM for 30 min at 37 °C and then stimulated with AA, 20 μM, for 30 min (at 37 °C), and TXB_2 production was determined in medium by RIA as an index of COX-1 activity (white bars). At the same time, other THP-1 cells were incubated with the different compounds at 100 μM and then washed twice with 10 mL of RPMI-1640 and finally centrifuged at 1200 rpm for 5 min. Thus, cells were then resuspended with medium and stimulated with AA, 20 μM, for 30 min, and TXB_2 production was determined in medium by RIA as an index of COX-1 activity (black bars). In panel B, results are depicted as the mean + SEM of percentage of control of TXB_2 levels in medium of AA-stimulated THP-1 from five to six separate experiments: (∗) $P < 0.05$, (∗∗)$P < 0.001$ versus without washing.

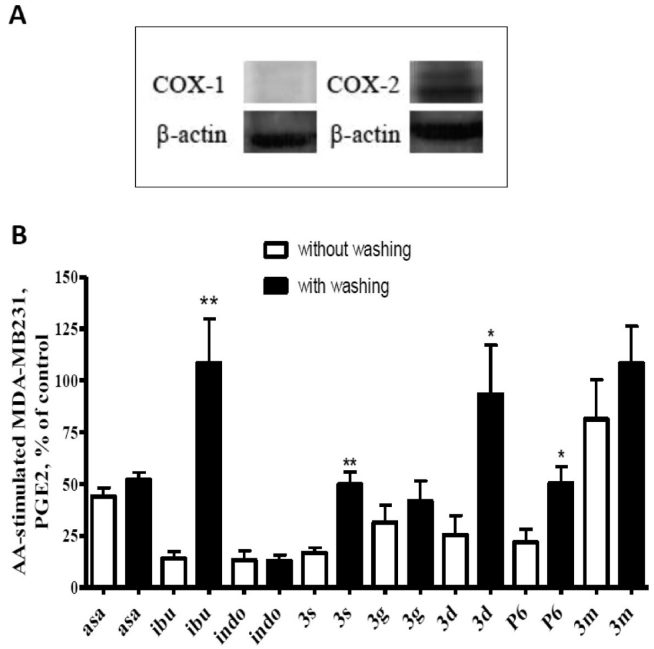

Figure 7. Assessment of the inhibition of COX-2 and its reversibility by diarylisoxazole derivatives in MDA-MB231 cells. Western blot analysis showed that MDA-MB231 expressed only COX-2 but not COX-1 (A). Before each experiment, cells were plated at a concentration of 1×10^6 in 5 cm plates (volume 3 mL) containing 2 mL of DMEM supplemented with 0.50% of FBS for 16 h. First, we assessed the inhibition of COX-2 activity by preincubating the cells with vehicle (DMSO) or with the different test compounds at a final concentration of 100 μM for 30 min (at room temperature) and then stimulating with AA, 0.50 μM, for a further 30 min (at 37 °C). In both experimental conditions [without (white bars) or with washing passages (black bars)], PGE_2 production was determined in medium by RIA as an index of COX-2 activity. In panel B, results are depicted as the mean + SEM of percentage of control of PGE_2 levels in medium of AA-stimulated MDA-MB231 from four to six separate experiments: (∗) $P < 0.05$, (∗∗) $P < 0.001$ versus without washing.

We assessed the inhibitory effects on COX-2 by 100 μM of the different compounds in MDA-MB231 cells cultured in a medium containing very low concentrations of proteins (0.50% FBS). The preincubation of ibuprofen, indomethacin, **3s**, **3g**, **3d**, and **6**, at 100 μM, with MDA-MB231 cells for 30 min caused a profound and significant inhibition of AA-induced PGE_2 generation that ranged from 86% to 70% (Figure 7B). This concentration of diarylisoxazole derivatives inhibited only marginally COX-2 activity in whole blood (Figure 1) because in this assay the presence of plasma proteins reduced the free drug fraction.

A lower degree of inhibition was caused by aspirin (60 ± 4%) which is consistent with previous results showing a lower potency of aspirin toward COX-2 than COX-1.[27,42] As shown in Figure 7B, **3m** did not significantly affect COX-2 activity.

The reversibility of the interaction between COX-2 and the different compounds was evaluated by assessing the recovery of COX-2 activity by washing the cells previously preincubated with them for 30 min. Similar to aspirin and indomethacin, the inhibition caused by **3g** was not significantly reversed by the washing procedure. In contrast, the inhibition caused by ibuprofen and **3d** was completely reversed. The inhibition of COX-2 activity by **3s** and **6** was only partially reversed by washing the cells (Figure 7B).

Altogether these results showed that the diarylisoxazole derivatives may affect COX-2 at high concentrations and this effect was caused by different mechanisms. **3d** resembles the mechanism of ibuprofen, i.e., quickly reversible inhibition of COX-2, thus suggesting a weak binding to COX-2. **3g** resembles the mechanism of indomethacin, i.e., slowly reversible inhibition, thus suggesting a strong binding to COX-2. **6** and **3s** were characterized by intermediate responses, thus suggesting that they bind COX-2 with lower affinity than **3g** but higher affinity than **3d**.

Effects of the Oral Administration of 3d on in Vivo Markers of COX-1 and COX-2 Activity in Mice. Among the novel diarylisoxazole derivatives, **3d** represents an interesting candidate for preclinical development as novel antithrombotic agent, and further studies are needed to assess its efficacy in animal models of thrombosis and atherosclerosis. Here we verified the capacity of the oral administration of **3d** [20 mg kg^{-1} day^{-1}, po, in 1% carboxymethylcellulose (CMC) solution given for 3 consecutive days to mice] to affect the systemic biosynthesis of TXA_2 by assessing the urinary levels of an enzymatic metabolite of TXB_2, i.e., 11-dehydro-TXB_2 (TX-M) which is mainly derived from platelet COX-1. In fact, its urinary levels are reduced by 70−80% in mice and humans after dosing with low-dose aspirin.[19,43] As shown in Figure 8A, **3d** caused a significant reduction (70%, $P = 0.0007$ versus CMC, $n = 4$) of the urinary levels of TX-M.

Moreover, we assessed the impact of **3d** administration on the urinary levels of PGI_2 (as assessed by the measurement of the

dx.doi.org/10.1021/jm301905a | J. Med. Chem. 2013, 56, 4277−4299

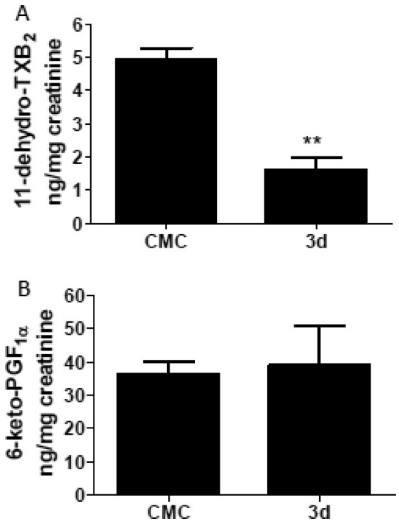

Figure 8. Biosynthesis of prostanoids in mice treated with **3d** or its vehicle (CMC). In 24 h urine collections performed after the third dose of **3d** (20 mg kg^{-1} day^{-1}, po) or CMC, we assessed urinary excretion of 11-dehydro-TXB_2, an enzymatic metabolite of TXB_2, as an index of systemic TXA_2 biosynthesis in vivo, mainly platelet COX-1-derived, and 6-keto-$PGF_{1\alpha}$ as an index of renal biosynthesis of PGI_2, mainly of COX-2-dependent origin. Data are expressed as the mean + SEM. Four mice were used for each group. Metabolite levels were corrected for urinary creatinine and expressed as ng/mg creatinine: (**) $P = 0.0007$ versus CMC using Student's t test.

nonenzymatic hydrolysis product 6-keto-$PGF_{1\alpha}$) which is a marker of renal biosynthesis of PGI_2, mainly derived from vascular COX-2.[44,45] As shown in Figure 8B, **3d** did not significantly affect the urinary excretion of PGI_2. Altogether these results showed that **3d** is effective also in vivo to affect the biosynthesis of the platelet agonist TXA_2 while sparing COX-2-dependent PGI_2. Vascular PGI_2 is a potent vasodilator, an inhibitor of platelet function, but it is also involved in the maintenance of cortical kidney functions.[46]

Docking Studies. To get a better comprehension of the high COX-1 inhibitory potency of the newly synthesized isoxazole derivatives at a molecular level and shed light on the structural determinants for their COX-1 specificity, docking experiments were conducted using the ovine COX-1 in complex with celecoxib (PDB code 3kk6).[47] Docking investigations were carried out through the automated docking program GOLD 5.0.1,[48] and the outcomes were rationalized using the clustering algorithm AclAP.[49] Alternative conformations of R120, Y355, and S530 have been previously observed in the COX crystal structures complexed with several inhibitors, highlighting the innate plasticity of the active site.[50−53] Accordingly, the side chains of R120, Y355, and S530 were allowed to move during the docking experiments.

We performed docking of **3s** and **3m** which may affect COX-1 activity by different mechanisms. In fact, pharmacological findings have shown that (i) **3s** inhibited COX-1 through a slowly reversible mechanism and (ii) **3m** inhibited COX-1 through a rapidly reversible mechanism. Docking of **3s** into the COX-1 active site revealed a very clear preference for two alternative poses (Figure 9). In the top-ranking pose A (GOLD fitness score of 58.70 kcal mol^{-1}), **3s** lies on the internal side of the constriction, at the base of the funnel-shaped entrance to the COX-1 active site (Figure 9a). The constriction, which consists of a H-bonding network formed by R120, E524, and Y355, is proposed to control the binding dynamics of some NSAIDs and selective COX-2 inhibitors.[54,55] Both O1 furan oxygen and N2 isoxazole nitrogen of the inhibitor are within H-bonding distance of the OH group of Y355. The O1···O and N2···O atoms are separated by 2.70 and 2.90 Å, respectively, and display a favorable geometry for H-bonding. The phenyl ring at position 4 of isoxazole forms hydrophobic interactions with I523, G526, and V349. Importantly, the 5-bromofuranyl moiety of **3s** is oriented toward the side pocket (residues 513−520) of COX-1 and makes hydrophobic contacts with residues H90, L352, I517, F518, and I523. In the second-ranking pose B (GOLD fitness score of 53.80 kcal mol^{-1}), **3s** is located at the apex of the COX-1 channel instead of near the opening (Figure 9b). The N2 isoxazole nitrogen and the O1 furan oxygen of the inhibitor engage a bifurcated H-bond with the γ-OH of S530, displaying a favorable geometry for H-bonding. The N···HO bond is stronger than O−H···O, the N2−O and O1−O distance being 2.50 and 2.90 Å, respectively. The phenyl ring at position 4 of isoxazole is in close contact with various hydrophobic side chains, including L352,

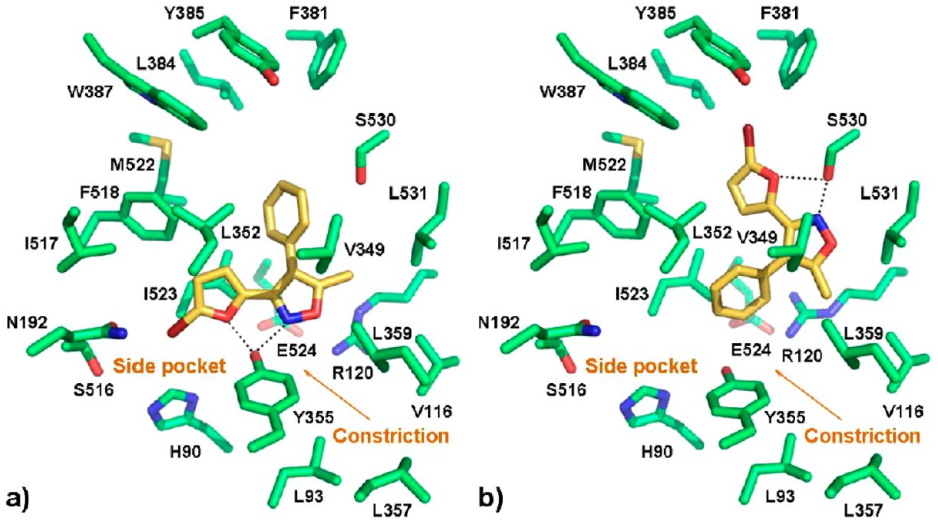

Figure 9. Binding mode A (a) and binding mode B (b) of compound **3s** (yellow) into the COX-1 binding site. Only amino acids located within 5 Å of the bound ligand are displayed and labeled. H-bonds discussed in the text are depicted as dashed black lines.

dx.doi.org/10.1021/jm301905a | J. Med. Chem. 2013, 56, 4277−4299

I523, and Y355. Interestingly, this phenyl group engages an edge-to-face interaction with Y355. The 5-methyl group is tucked into a small hydrophobic cleft lined by V349, L359, V116, and L531 residues. Finally, the 5-bromofuranyl moiety of **3s** is oriented toward the apex of the COX-1 active site and forms van der Waals interactions with residues M522, F518, L352, W387, Y385, L384, F381.

When the inhibitor **3m** was docked into the COX-1 binding pocket, only 10% of the generated conformations adopted the above-described binding mode B of **3s** (Figure 9a), whereas 90% were located at the base of the active site. As illustrated in Figure 10, the N2 isoxazole nitrogen of the inhibitor makes a H-bond

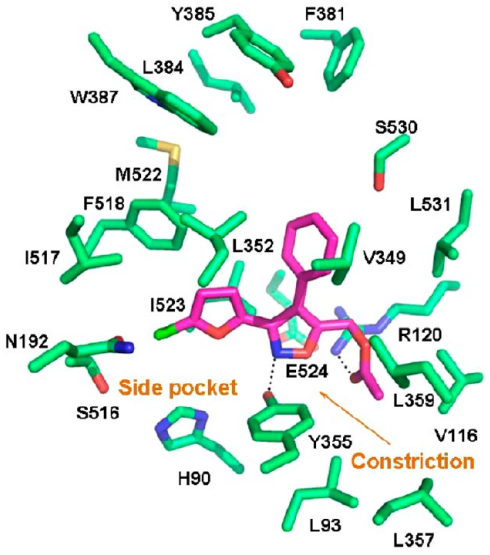

Figure 10. Compound **3m** (magenta) docked into the COX-1 binding site. Only amino acids located within 5 Å of the bound ligand are displayed and labeled. H-bonds discussed in the text are depicted as dashed black lines.

with the OH group of Y355, while the C═O oxygen of the 5-acetoxy substituent establishes a H-bond with the guanidinium group of R120 typically seen with substrates and carboxylic acid containing inhibitors. The 4-phenyl ring and the 5-chlorofuranyl moiety of **3m** insert into the hydrophobic pocket framed by I523, G526, and V349 and the side pocket, respectively. Taken together, these results suggest a rationale for the different kinetic behavior of the COX-1 inhibitors, **3s**, and **3m**.

Recent evidence suggest that both COX-1 and COX-2 exhibit half of site COX activity (i.e., the COX active site of only one monomer of a COX dimer can function at a given time)[56,57] and that the enzymes function as an allosteric/catalytic couple in which one COX active site has a catalytic function (E_{cat}) that is modulated by the nature of the ligand occupying the COX site of the partner, allosteric monomer (E_{allo}).[47,52,56,58,59] This conclusion comes from the recent discovery that the two subunits communicate through the dimer interface.[56] Time-independent COX inhibitors compete reversibly with the natural substrate to form a complex enzyme−inhibitor (EI). These inhibitors can function by binding E_{allo} and E_{cat}.[60] On the contrary, time-dependent COX inhibitors are generally imagined as functioning in two steps, although there may be a third step with some inhibitors.[40] The first step is a rapid, reversible binding to the COX active site of either E_{allo} or E_{cat} to form a complex (EI). The second step involves a slow conformational change to a tightly bound complex (EI*). The latter process occurs in seconds or minutes and is even more slowly reversible.[40,61,62]

On the basis of our docking results, it is possible to speculate that the binding mode A of the time-dependent inhibitor **3s** represents the initial enzyme−inhibitor complex (EI), where the channel H-bonding network of R120, Y355, and E524 is perturbed by the interaction between the inhibitor and Y355 residue (binding mode A, Figure 9b). Additional protein conformational changes may also occur as part of this process. Crystal structures of NSAIDs bound to COX-1 and COX-2 demonstrate that protein conformational changes must occur during or after the binding of the inhibitor in the COX active site.[50,63]

A rearrangement of the inhibitor in the active site ultimately results in a stable complex with S530 residue (binding mode B, Figure 9b), which represents the enzyme−inhibitor complex (EI*). This model is consistent with a time-dependent inhibition mechanism as observed experimentally. Support for this model comes from fluorescence studies of holo-COX-2, which suggest that for a time-dependent inhibitor, EI and EI* correspond to inhibitor binding at distinct sites.[64]

3m also disturbs the H-bond network in the constriction region of COX-1 engaging H-bonds with Y355 and R120, and it is consequently expected that the inhibitor forms a tight complex in the COX binding site that could represent the EI state (Figure 10). Its status as relatively weak, rapidly reversible COX inhibitor might be derived from the fact that **3m** has to bind to both subunits E_{allo} and E_{cat} of COX-1 to inhibit productive binding of AA and that binding in the second subunit is competitive with AA.

■ CONCLUSIONS

Structural features of the highly selective COX-1 inhibitor 3-(5-chlorofuran-2-yl)-5-methyl-4-phenylisoxazole (**6**)[31] have been used to design a new series of diarylisoxazoles. By use of the human whole blood assays in vitro, the SAR study has evidenced that the simultaneous presence of (i) 5-methyl, (ii) 4-phenyl, and (iii) 5-chlorofuran-2-yl groups on the isoxazole core is crucial to obtain selective inhibition of COX-1. The replacement of the chloro atom in the furyl core of **6** with the bromo atom or with the methyl group (i.e., **3s** and **3g**, respectively) and the introduction of a CF_3 group in place of the 5-methyl group of **6** (i.e., **3d**) led to compounds that bind more tightly COX-1, and its inhibition is slowly reversible. This translated into an improved potency to inhibit platelet aggregation in response to AA and collagen, which occurs as a consequence of the rapid generation of TXA_2 from elevated concentration of free AA. We synthesized the acetoxy derivative of **6** (**3m**) with the aim to acetylate COX isozymes similarly to aspirin. However, this compound was not able to cause an irreversible inhibition of COX-1 and COX-2 but similar to **6** was a reversible competitive inhibitor of COX-1, and this mechanism of inhibition translated into a lower efficacy to inhibit platelet function than the other diarylisoxazole derivatives.

Molecular docking provided insight into the binding modes of **3s** and **3m** into the COX-1 binding site and rationalized their different kinetic inhibition mechanisms.

Among the novel diarylisoxazole derivatives that we have synthesized, **3d** represents a candidate for preclinical development as a novel antithrombotic agent. It is >1000-fold more potent to inhibit COX-1 than COX-2, showing a different mechanism of interaction with the two COX-isozymes, i.e., a strong, slowly reversible interaction with COX-1 and a rapidly

reversible one with COX-2. The potency of this compound to inhibit human platelet aggregation correlated with its capacity to inhibit the generation of TXA_2 in response to proaggregatory stimuli, supporting its mechanism of action as antiplatelet agent through the inhibition of platelet COX-1. The oral administration of **3d** to mice caused a selective inhibitory effect on TXB_2 in vivo (mainly COX-1-derived) while sparing PGI_2 (mainly COX-2-derived). These results may implicate the induction of a protective phenotype for the CV system by this compound, which needs to be confirmed in appropriate animal models.

EXPERIMENTAL SECTION

Chemistry. Melting points taken on an Electrothermal apparatus were uncorrected. ^{1}H NMR and ^{13}C NMR spectra were recorded on a Varian-Mercury 300 MHz, on a Varian-Inova 400 MHz spectrometer, and on a Bruker-Aspect 3000 console 500 MHz spectrometer, and chemical shifts are reported in parts per million (δ). ^{19}F NMR spectra were recorded by using $CFCl_3$ as internal standard. Absolute values of the coupling constant are reported. FT-IR spectra were recorded on a Perkin-Elmer 681 spectrometer. GC analyses were performed by using a HP1 column (methyl siloxane; 30 m × 0.32 mm × 0.25 μm film thickness) on a HP 6890 model, series II instrument. Thin-layer chromatography (TLC) was performed on silica gel sheets with fluorescent indicator. The spots on the TLC were observed under ultraviolet light or were visualized by I_2 vapor. Chromatography was conducted by using silica gel 60 with a particle size distribution of 40−63 μm and 230−400 ASTM. GC−MS analyses were performed on an HP 5995C instrument and elemental analyses on an elemental analyzer 1106-Carlo Erba instrument. MS-ESI analyses were performed on Agilent 1100 LC/MSD trap system VL. All synthesized compounds were analyzed by CHN or by HPLC analysis performed on an Agilent 1260 Infinity instrument equipped with a 1260 DAD VL+ detector, and their purity is higher than 95%.

Materials. Tetrahydrofuran (THF) from a commercial source was purified by distillation (twice) from sodium wire under nitrogen. Dichloromethane from a commercial source was purified by distillation from CaH_2 under nitrogen atmosphere. DMF from a commercial source was purified by distillation from CaH_2 under reduced pressure. Standardized (2.50 M) *n*-butyllithium in hexanes was purchased from Aldrich Chemical Co., and its titration was performed with *N*-pivaloyl-*o*-toluidine.[65] Diisopropylamine from a commercial source was purified by distillation from CaH_2 under reduced pressure and nitrogen atmosphere. All other chemicals and solvents of commercial grade were further purified by distillation or crystallization prior to use. Arylnitrile oxides were prepared from aldehydes through their conversion to the corresponding oximes and then to benzohydroximinoyl chlorides.[31,66] These were finally converted into nitrile oxides by treatment with NEt_3, followed by vacuum filtration of NEt_3·HCl from the solution.[67] Oximes, prepared from reaction of aldehydes/EtOH and NH_2OH·HCl/aqueous NaOH, had analytical and spectroscopic data identical to those previously reported or commercially available.[68−71]

General Procedure for the Synthesis of 5-Alkyl-3,4-diaryl-5-hydroxy-2-isoxazolines 2a−g by Reaction of Arylnitrile Oxides with Enolate Ion of 3-Aryl-2-propanones 1a−d (Table 1). A solution of the 3-aryl-2-propanones **1a−d** (105 mg, 0.558 mmol) in THF (3 mL) was dropwise added to a suspension of NaH (95% w/w, 28.20 mg, 1.116 mmol) in THF (6 mL) at 0 °C under nitrogen atmosphere, using a nitrogen-flushed, three-necked flask equipped with a magnetic stirrer, a nitrogen inlet, and two dropping funnels.[72] After the yellow mixture had been stirred for 1 h, a solution of arylnitrile oxide (0.558 mmol) in THF (3 mL) was added. The reaction mixture was allowed to reach room temperature and stirred overnight and then quenched by adding aqueous NH_4Cl solution. The reaction products were extracted three times with ethyl acetate. The organic phase was dried over anhydrous Na_2SO_4 and then evaporated under vacuum. Column chromatography (silica gel, petroleum ether/ethyl acetate = 15/1) of the residue affords the 5-alkyl-3,4-diaryl-5-hydroxy-2-isoxazolines **2a−g** in 23−71% yield (Table 2).

3-(3-Chlorophenyl)-5-hydroxy-5-methyl-4-phenyl-2-isoxazoline (2a). 71% yield. Mp 124.50−128.40 °C (diastereoisomeric mixture). FT-IR (KBr): 3600−3150, 3078, 3026, 3005, 2987, 2940, 1591, 1561, 1490, 1455, 1409, 1383, 1355, 1339, 1265, 1229, 1139, 1094, 1044, 925, 887, 873, 809, 802, 750, 700, 679 cm^{-1}. ^{1}H NMR (300 MHz, $CDCl_3$, δ): 7.80−7.77 (m, 1H, aromatic proton, minor isomer); 7.67−7.64 (m, 1H, aromatic proton, major isomer); 7.43−7.01 (m, 8H, aromatic protons for each stereoisomer); 4.50 (s, 1H, major isomer); 4.40 (s, 1H, minor isomer); 3.35−3.26 (bs, 1H, OH exchanges with D_2O; 1H major isomer); 2.30−2.10 (bs, 1H, OH exchanges with D_2O; 1H minor isomer); 1.77 (s, 3H, minor isomer); 1.27 (s, 3H, major isomer). ^{13}C NMR (75 MHz, $CDCl_3$, δ): 159.90, 134.90, 134.30, 130.90, 130.40, 130.20, 130.10, 130.10, 129.80, 129.60, 129.20, 128.60, 127.40, 127.10, 125.70, 125.40, 63, 60.70, 22.40. GC−MS (70 eV) *m*/*z* (rel intens): 287 (M$^+$, 0.70), 269 (18), 229 (35), 228 (26), 227 (100), 226 (9), 193 (9), 192 (15), 165 (23), 137 (17), 134 (9), 116 (15), 91 (17), 90 (30), 89 (34), 77 (9), 75 (12), 43 (26). Anal. Calcd for $C_{16}H_{14}ClNO_2$: C, 66.79; H, 4.90; N, 4.87. Found: C, 66.70; H, 4.93; N, 4.81.

3-(5-Chlorofuran-2-yl)-5-hydroxy-5-(trifluoromethyl)-4-phenyl-2-isoxazoline (2d). 71% yield. FT-IR (KBr): 3600−3150, 3037, 2924, 2852, 1616, 1494, 1457, 1324, 1244, 1174, 1086, 1041, 1018, 946, 857, 790, 701 cm^{-1}. ^{1}H NMR (300 MHz, $CDCl_3$, δ): 7.45−7.43 (m, 3H, aromatic protons, major isomer); 7.34−7.32 (m, 3H, aromatic protons, minor isomer); 7.27−7.24 (m, 2H, aromatic protons for each stereoisomer); 6.44−6.43 (d, J = 3.60 Hz, 1H, furylic proton, minor isomer); 6.23−6.22 (d, J = 3.60 Hz, 1H, furylic proton, major isomer); 6.17−6.16 (d, J = 3.60 Hz, 1H, furylic proton, minor isomer); 6.14−6.13 (d, J = 3.60 Hz, 1H, furylic proton, major isomer); 4.91 (s, 1H, major isomer); 4.78 (s, 1H, minor isomer); 3.42−3.30 (bs, 2H, OH exchanges with D_2O; 1H for each stereoisomer). ^{13}C NMR (75 MHz, $CDCl_3$, δ): 150.50, 142.60, 140.40, 129.90, 129.70, 129.40, 129.10, 122.30 (q, $^1J_{19F\text{-}13C}$ = 285 Hz), 116.60, 108.90 (minor diastereoisomer), 108.80 (major diastereoisomer), 103.90 (q, $^2J_{19F\text{-}13C}$ = 33.50 Hz), 57.70. GC−MS (70 eV) *m*/*z* (rel intens): 331 (M$^+$, 92), 216 (24), 188 (100), 139 (20), 127 (7), 102 (31), 89 (22), 77 (25), 63 (2), 51 (9). Anal. Calcd for $C_{14}H_9ClF_3NO_3$: C, 50.70; H, 2.74; N, 4.22. Found: C, 50.48; H, 2.60; N, 4.20.

3-(5-Chlorofuran-2-yl)-4-(2-fluorophenyl)-5-hydroxy-5-methyl-2-isoxazoline (2e). 56% yield. Mp 130−131 °C. FT-IR (KBr): 3590−3200, 3131, 2964, 1613, 1582, 1547, 1490, 1458, 1387, 1378, 1229, 1206, 1145, 1100, 1015, 915, 901, 789, 758 cm^{-1}. ^{1}H NMR (300 MHz, $CDCl_3$, δ): 7.40−6.90 (m, 8H, four aromatic protons of each stereoisomer); 6.51 (d, J = 3.6 Hz, 1H, cis diastereoisomer); 6.17 (d, J = 3.60 Hz, 2H, one furyl proton of the cis diastereoisomer and one of the trans); 6.12 (d, J = 3.60 Hz, 1H, furyl proton, trans diastereoisomer); 4.84 (s, 2H, isoxazoline protons, 1H of each diastereoisomer); 3.36 (bs, 1H, OH exchanges with D_2O; proton of cis diastereoisomer); 3.15−2.80 (bs, 1H, OH exchanges with D_2O, proton of trans diastereoisomer); 1.78 (s, 3H, CH_3 of trans diastereoisomer); 1.33 (s, 3H, CH_3 of cis diastereoisomer). ^{13}C NMR (75 MHz, $CDCl_3$, δ): 160.50 (d, $^1J_{19F\text{-}13C}$ = 247.40 Hz), 152.10, 143.90 (minor diastereoisomer), 143.70 (major diastereoisomer), 139.80 (major diastereoisomer), 139.70 (minor diastereoisomer), 131.30, 130.70 (d, $^3J_{19F\text{-}13C}$ = 8.90 Hz, minor diastereoisomer), 130.40 (d, $^3J_{19F\text{-}13C}$ = 8.30 Hz, major diastereoisomer), 129.20, 125.20 (d, $^4J_{19F\text{-}13C}$ = 3.80 Hz, major diastereoisomer), 124.80 (minor diastereoisomer), 121.40 (d, $^2J_{19F\text{-}13C}$ = 14.50 Hz, minor diastereoisomer), 116.10 (d, $^2J_{19F\text{-}13C}$ = 22.00 Hz, major diastereoisomer), 115.50 (major diastereoisomer), 115.10 (minor diastereoisomer), 108.90 (d, $^2J_{19F\text{-}13C}$ = 24.70 Hz, major diastereoisomer), 108.40 (d, $^2J_{19F\text{-}13C}$ = 16.90 Hz, minor diastereoisomer), 66.20 (minor diastereoisomer), 54.60 (major diastereoisomer), 25.70 (minor diastereoisomer), 21.40 (major diastereoisomer). GC−MS (70 eV) *m*/*z* (rel intens): 297 [(M$^+$ + 2), 10], 295 (M$^+$, 26), 278 (22), 253 (20), 237 (11), 236 (19), 235 (22), 234 (13), 209 (12), 206 (15), 200 (12), 173 (19), 172 (100), 157 (13), 145 (13), 133 (10), 120 (11), 109 (13), 107 (13), 43 (25). Anal. Calcd for $C_{14}H_{11}ClFNO_2$: C, 56.87; H, 3.75; N, 4.74. Found: C, 56.84; H, 3.72; N, 4.75.

3-(5-Chlorofuran-2-yl)-4-(4-fluorophenyl)-5-hydroxy-5-methyl-2-isoxazoline (2f). 62% yield. Mp 101−102 °C. FT-IR (KBr): 3580−3100, 3050, 2999, 2926, 1602, 1512, 1495, 1442, 1392, 1374, 1318, 1233, 1126, 1014, 945, 917, 898, 828, 786 cm^{-1}. ^1H NMR (300 MHz, $CDCl_3$, δ): 7.30−7.00 (m, 8H, four aromatic protons for each stereoisomer); 6.47 (d, J = 3.50 Hz, 1H, furyl proton, cis diastereoisomer); 6.15 (d, J = 3.50 Hz, 1H, furyl proton, cis diastereoisomer); 6.12 (d, J = 3.50 Hz, 1H, furyl proton, trans diastereoisomer); 6.09 (d, J = 3.50 Hz, 1H, furyl proton, trans diastereoisomer); 4.40 (s, 1H, cis isoxazoline proton); 4.36 (s, 1H, trans isoxazoline proton); 1.75 (s, 3H, CH_3 of trans diastereoisomer); 1.28 (s, 3H, CH_3 of cis diastereoisomer). ^{13}C NMR (125 MHz, $CDCl_3$, δ): 167, 162.70 (d, $^1J_{19F\text{-}13C}$ = 248.10 Hz), 152.10, 143.40, 138.50 (major diastereoisomer), 138.40 (minor diastereoisomer),131.70 (d, $^3J_{19F\text{-}13C}$ = 8.10 Hz, major diastereoisomer), 130.90 (d, $^3J_{19F\text{-}13C}$ = 8 Hz, minor diastereoisomer), 125.30 (d, $^4J_{19F\text{-}13C}$ = 3.30 Hz, major diastereoisomer), 115.90 (d, $^2J_{19F\text{-}13C}$ = 21.70 Hz, major diastereoisomer), 115.60 (d, $^2J_{19F\text{-}13C}$ = 21.40 Hz, minor diastereoisomer), 115, 113.80 (minor diastereoisomer), 113.40 (major diastereoisomer), 108.40 (minor diastereoisomer), 107.90 (major diastereoisomer), 62, 49.90, 11.10. GC−MS (70 eV) m/z (rel intens): 297 [(M^+ + 2), 7], 295 (M^+, 18), 237 (12), 236 (21), 235 (25), 234 (13), 206 (13), 200 (13), 173 (19), 172 (100), 157 (11), 145 (11), 120 (12), 109 (11), 107 (12), 43 (17). Anal. Calcd for $C_{14}H_{11}ClFNO_2$: C, 56.87; H, 3.75; N, 4.74. Found: C, 56.80; H, 3.74; N, 4.71.

5-Hydroxy-5-methyl-3-(5-methylfuran-2-yl)-4-phenyl-2-isoxazoline (2g). 23% yield. Mp 121.50−123.40 °C (diastereoisomeric mixture). FT-IR (KBr): 3478, 3117, 3084, 3028, 3005, 2989, 2956, 2924, 2847, 1613, 1574, 1518, 1496, 1454, 1385, 1237, 1209, 1149, 1083, 1021, 950, 911, 886, 871, 791, 753, 700 cm^{-1}. ^1H NMR (400 MHz, $CDCl_3$, δ): 7.38−7.26 (m, 3H, aromatic protons for each stereoisomer); 7.25−7.13 (m, 2H, aromatic protons for each stereoisomer); 6.30 (d, J = 3.30 Hz, 1H, furylic proton, major isomer); 5.96 (d, J = 3.60 Hz, 1H, furylic proton, minor isomer); 5.93 (d, J = 3.30 Hz, 1H, furylic proton, major isomer); 5.90 (d, J = 3.60 Hz, 1H, furylic proton, minor isomer); 4.38 (s, 1H, major isomer); 4.33 (s, 1H, minor isomer); 3.62−3.52 (bs, 1H, OH exchanges with D_2O); 2.28 (s, 3H protons for each stereoisomer); 1.74 (s, 3H, minor isomer); 1.26 (s, 3H, major isomer). ^{13}C NMR (100 MHz, $CDCl_3$, δ): 155.10 (major isomer), 155 (minor isomer), 153 (major isomer), 152.06 (minor isomer), 142.60 (minor isomer), 142.50 (major isomer), 134.70 (major isomer), 132.20 (minor isomer), 129.30, 129, 128.90, 128.50, 128, 115 (major isomer), 114.90 (minor isomer), 108.70, 107.90, 107.72, 107.71, 63.20 (major isomer), 61.10 (minor isomer), 25.70 (minor isomer), 21.80 (major isomer), 13.70 (major isomer), 13.68 (minor isomer). GC−MS (70 eV) m/z (rel intens): 257 (M^+, 23), 240 (18), 239 (38), 198 (28), 197 (100), 196 (26), 182 (8), 171 (9), 168 (9), 155 (7), 154 (22), 115 (8), 102 (41), 89 (9), 43 (131). Anal. Calcd for $C_{15}H_{15}NO_3$: C, 70.02; H, 5.88; N, 5.44. Found: C, 69.98; H. 5.89; N, 5.46.

General Procedure for the Synthesis of Isoxazoles 3a−g from 5-Alkyl-3,4-diaryl-5-hydroxy-2-isoxazolines 2a−g.[67] A solution of Na_2CO_3 (70 mg, 0.568 mmol) in water (3 mL) was added to a solution of the 5-alkyl-3,4-diaryl-5-hydroxy-2-isoxazoline **2a−g** (94 mg, 0.284 mmol) in THF (10 mL). The reaction mixture was then heated under reflux (reaction time reported in Scheme 1). The two phases were separated, and the aqueous layer was extracted three times with ethyl acetate. The combined organic extracts were dried over anhydrous Na_2SO_4, and the solvent evaporated under reduced pressure. Column chromatography (silica gel, petroleum ether/ethyl acetate = 19/1) of the residue affords the 5-alkyl-3,4-diarylisoxazoles in 42−90% yield (Table 2).

3-(3-Chlorophenyl)-5-methyl-4-phenylisoxazole (3a). 72% yield (100 mg). Mp 85−88 °C (hexane), white powder. FT-IR (KBr): 3079, 3065, 3028, 2920, 1633, 1598, 1570, 1494, 1453, 1426, 1397, 1370, 1299, 1234, 1178, 1132, 1091, 1074, 1042, 1018, 975, 914, 897, 790, 757, 688 cm^{-1}. ^1H NMR (300 MHz, $CDCl_3$, δ): 7.52−7.48 (m, 1H, aromatic protons); 7.44−7.30 (m, 4H, aromatic protons); 7.28−7.14 (m, 4H, aromatic protons); 2.45 (s, 3H). ^{13}C NMR (75 MHz, $CDCl_3$, δ): 167.20, 160.20, 134.70, 131.10, 130.10, 123, 129.90, 129.70, 129.10, 128.60, 128.10, 126.80, 116, 11.80. GC−MS (70 eV) m/z (rel intens): 271 [(M^+ + 2), 37], 270 [(M^+ + 1), 21], 269 (M^+, 9), 256 (9), 254 (25), 229 (35), 228 (23), 227 (97), 226 (20), 191 (9), 190 (11), 165 (21), 103 (14), 89 (41), 77 (8), 75 (11), 63 (12), 43 (19). Anal. Calcd for $C_{16}H_{12}ClNO$: C, 71.25; H, 4.48; N, 5.19. Found: C, 70.98; H, 4.60; N, 5.20.

3-(2-Chlorophenyl)-5-methyl-4-phenylisoxazole (3b). Yellow solid. FT-IR (KBr): 3431, 3070, 1624, 1599, 1491, 1435, 1413, 1312, 1234, 1125, 1058, 1017, 963, 910, 768, 724, 696, 678, 572, 519, 460 cm^{-1}. ^1H NMR (400 MHz, $CDCl_3$, δ): 7.42−7.25 (m, 7H, aromatic protons); 7.09−7.06 (m, 2H, aromatic protons); 2.55 (s, 3H). ^{13}C NMR (100 MHz, $CDCl_3$, δ): 165.80, 160.60, 133.80, 131.70, 130.70, 130.10, 129.90, 128.80, 128.60, 127.30, 126.70, 117.10, 11.80. GC−MS (70 eV) m/z (rel intens): 271 [(M^+ + 2), 32], 269 (M^+, 93), 254 (28), 229 (34), 228 (21), 227 (100), 226 (21), 192 (9), 191 (9), 190 (14), 165 (19), 103 (9), 89 (41), 75 (7), 63 (8), 43 (9). Anal. Calcd for $C_{16}H_{12}ClNO$: C, 71.25; H, 4.48; N, 5.19. Found: C, 70.74; H, 4.50; N, 5.07.

3-(2-Chlorophenyl)-4-(2-fluorophenyl)-5-methylisoxazole (3c). Colorless semisolid. FT-IR (KBr): 3059, 3033, 2953, 2924, 2852, 1630, 1607, 1579, 1516, 1492, 1437, 1414, 1376, 1315, 1268, 1240, 1212, 1159, 1136, 1105, 1059, 1018, 965, 904, 818, 764, 753, 745, 734, 796, 664 cm^{-1}. ^1H NMR (400 MHz, $CDCl_3$, δ): 7.44−7.41 (m, 1H, aromatic proton); 7.35−7.24 (m, 4H, aromatic protons); 7.09−6.93 (m, 3H, aromatic protons); 2.48 (d, 3H, J = 1.50 Hz). ^{13}C NMR (100 MHz, $CDCl_3$, δ): 167.30, 159.80 (d, $^1J_{19F\text{-}13C}$ = 247.50 Hz), 133.50, 131.60, 131.10 (d, $^4J_{19F\text{-}13C}$ = 3 Hz), 130.70, 129.80, 129.70 (d, $^3J_{19F\text{-}13C}$ = 8.40 Hz), 128.50, 126.70, 124.10 (d, $^3J_{19F\text{-}13C}$ = 3.60 Hz), 117.80 (d, $^2J_{19F\text{-}13C}$ = 15.60 Hz), 115.90 (d, $^2J_{19F\text{-}13C}$ = 22 Hz), 111.50, 11.90 (d, $^5J_{19F\text{-}13C}$ = 3.60 Hz). GC−MS (70 eV) m/z (rel intens): 289 [(M^+ + 2), 24], 287 (M^+, 69), 272 (13), 247 (34), 246 (20), 245 (100), 244 (14), 210 (7), 208 (9), 183 (14), 107 (34), 75 (6), 43 (8). Anal. Calcd for $C_{16}H_{11}ClFNO$: C, 66.79; H, 3.85; N, 4.87. Found: C, 66.78; H, 4.00; N, 4.90.

3-(5-Chlorofuran-2-yl)-4-phenyl-5-(trifluoromethyl)-isoxazole (3d). 65% yield. Mp 55−57 °C. FT-IR (neat): 3147, 3064, 2925, 2853, 1608, 1517, 1493, 1446, 1415, 1355, 1315, 1260, 1210, 1196, 1160, 1148, 1073, 1023, 992, 968, 943, 899, 775, 700 cm^{-1}. ^1H NMR (300 MHz, $CDCl_3$, δ): 7.51−7.48 (m, 3H, aromatic protons); 7.34−7.32 (m, 2H, aromatic protons); 6.17 (d, J = 3.50 Hz, 1H, furyl proton); 6.15 (d, J = 3.50 Hz, 1H, furyl proton). ^{13}C NMR (75 MHz, $CDCl_3$, δ): 155 (q, $^2J_{19F\text{-}13C}$ = 40.40 Hz), 153.60, 141.80, 139.90, 129.90, 129.10, 125.90, 118.30 (q, $^1J_{19F\text{-}13C}$ = 270 Hz), 119.40, 115.50, 108.50. GC−MS (70 eV) m/z (rel intens): 315 [(M^+ + 2), 37], 313 (M^+, 100), 250 (13), 244 (15), 216 (22), 190 (23), 189 (11), 188 (64), 153 (22), 152 (19), 129 (20), 127 (12), 89 (20), 77 (6), 73 (10). Anal. Calcd for $C_{14}H_7ClF_3NO_2$: C, 53.61; H, 2.45; N, 4.46. Found: C, 53.60; H, 2.47; N, 4.41.

3-(5-Chlorofuran-2-yl)-4-(2-fluorophenyl)-5-methylisoxazole (3e). 90% yield. FT-IR (neat): 3144, 3067, 2928, 2854, 1639, 1604, 1580, 1521, 1495, 1455, 1436, 1417, 1208, 1137, 1108, 1021, 989, 943, 923, 899, 789, 763 cm^{-1}. ^1H NMR (400 MHz, $CDCl_3$, δ): 7.43−7.37 (m, 1H, aromatic proton); 7.27−7.14 (m, 3H, aromatic protons); 6.31 (d, J = 3.60 Hz, 1H, furyl proton); 6.13 (d, J = 3.60 Hz, 1H, furyl proton); 2.34 (s, 3H, CH_3). ^{13}C NMR (100 MHz, $CDCl_3$, δ): 167.80, 160.20 (d, $^1J_{19F\text{-}13C}$ = 247.9 Hz), 152.40, 143.30, 138.30, 132.10 (d, $^4J_{19F\text{-}13C}$ = 2.70 Hz), 130.60 (d, $^3J_{19F\text{-}13C}$ =8 Hz), 124.30 (d, $^3J_{19F\text{-}13C}$ =3.80 Hz), 117 (d, $^2J_{19F\text{-}13C}$ = 16 Hz), 115.90 (d, $^2J_{19F\text{-}13C}$ =21.70 Hz), 113, 108.30, 107.90, 11.20 (d, $^5J_{19F\text{-}13C}$ = 0.80 Hz). GC−MS (70 eV) m/z (rel intens): 279 [(M^+ + 2), 21], 277 (M^+, 57), 237 (36), 236 (20), 235 (100), 234 (14), 206 (11), 172 (49), 171 (18), 145 (19), 43 (15). Anal. Calcd for $C_{14}H_9ClFNO_2$: C, 60.56; H, 3.27; N, 5.04. Found: C, 60.60; H, 3.30; N, 5.06.

3-(5-Chlorofuran-2-yl)-4-(4-fluorophenyl)-5-methylisoxazole (3f). 90% yield. Mp 103.70−105.20 °C. FT-IR (KBr): 3147, 3077, 2931, 1637, 1595, 1522, 1508, 1445, 1418, 1403, 1236, 1230, 1223, 1203, 1158, 1135, 1018, 987, 939, 921, 896, 846, 794 cm^{-1}. ^1H NMR (500 MHz, $CDCl_3$, δ): 7.28−7.26 (m, 2H, aromatic protons); 7.16−7.13 (m, 2H, aromatic protons); 6.29 (d, J = 3.50 Hz, 1H, furyl proton); 6.15 (d, J = 3.50 Hz, 1H, furyl proton); 2.37 (s, 3H, CH_3). ^{13}C NMR (125 MHz, $CDCl_3$, δ): 167, 162.60 (d, $^1J_{19F\text{-}13C}$ = 247.90 Hz), 152.20, 143.30, 138.50, 131.70 (d, $^3J_{19F\text{-}13C}$ =8.60 Hz), 125.30 (d, $^4J_{19F\text{-}13C}$ =2.90 Hz), 115.80 (d, $^2J_{19F\text{-}13C}$ =21 Hz), 113.80, 113.50, 107.90, 11.17. GC−MS (70

dx.doi.org/10.1021/jm301905a | J. Med. Chem. 2013, 56, 4277−4299

eV) m/z (rel intens): 279 (M^+ + 2), 16), 277 (M^+, 49), 237 (35), 236 (19), 235 (100), 234 (12), 206 (12), 172 (46), 171 (20), 170 (11), 147 (16), 145 (20), 89 (13), 43 (30). Anal. Calcd for $C_{14}H_9ClFNO_2$: C, 60.56; H, 3.27; N, 5.04. Found: C, 60.58; H, 3.24; N, 5.01.

5-Methyl-3-(5-methylfuran-2-yl)-4-phenylisoxazole (3g). 65% yield. Yellow oil. FT-IR (KBr): 3058, 2924, 2852, 1627, 1598, 1566, 1498, 1435, 1300, 1239, 1208, 1149, 1074, 1024, 922, 898, 791, 772, 701 cm^{-1}. ^1H NMR (400 MHz, $CDCl_3$, δ): 7.44−7.40 (m, 3H, aromatic protons); 7.31−7.24 (m, 2H, aromatic protons); 6.12 (d, 1H, J = 3.30 Hz, furylic proton); 5.94−5.92 (m, 1H, furylic proton); 2.36 (s, 3H), 2.32 (s, 3H). ^{13}C NMR (100 MHz, $CDCl_3$, δ): 166.30, 153.90, 153, 142.20, 130.10, 130, 128.60, 128.10, 114.10, 112.80, 107.30, 13.60, 11.20. GC−MS (70 eV) m/z (int. rel.): 239 (M^+, 48), 198 (15), 197 (100), 196 (23), 168 (5), 167 (6), 154 (7), 129 (7), 127 (5), 115 (5), 89 (4), 43 (7), 102 (10), 261 (100), 234 (10), 232 (10), 154 (54), 153 (33), 129 (12), 127 (31), 77 (9), 43 (14). Anal. Calcd for $C_{15}H_{13}NO_2$: C, 75.30; H, 5.48; N, 5.85. Found: C, 75.08; H, 5.60; N, 5.90.

Synthesis of 3-(Furan-2-yl)-5-methyl-4-phenylisoxazole (3q) and 5-Methyl-4-phenyl-3-(tetrahydrofuran-2-yl)isoxazole (3r). A solution of 3-(5-chlorofuran-2-yl)-5-methyl-4-phenylisoxazole (0.097g, 0.374 mmol) in EtOH (2 mL) was hydrogenated over Adams catalyst (0.005g, 0.022 mmol) at room temperature and atmospheric pressure for 6 h in a round-bottom flask equipped with magnetic stirring. The catalyst was removed by filtration, and the solution was concentrated in vacuo. Column chromatography (silica gel, petroleum ether/ethyl acetate = 12/1) of the residue affords the 3-(furan-2-yl)-5-methyl-4-phenylisoxazole (**3q**) in 89% yield as a white solid and the 5-methyl-4-phenyl-3-(tetrahydrofuran-2-yl)isoxazole (**3r**) in 16% yield as a colorless semisolid.

3-(Furan-2-yl)-5-methyl-4-phenylisoxazole (3q). 89% yield. Mp 93−96 °C (hexane). White powder. FT-IR (KBr): 3149, 3122, 3059, 2962, 2925, 2853, 1633, 1605, 1511, 1496, 1448, 1438, 1417, 1239, 1225, 1176, 1070, 1020, 976, 923, 891, 782, 714, 700 cm^{-1}. ^1H NMR (400 MHz, $CDCl_3$, δ): 7.47−7.41 (m, 4H, aromatic protons); 7.31−7.28 (m, 2H, aromatic protons); 6.37−6.35 (dd, 1H, J = 3.30 Hz, J = 1.80 Hz, furylic proton); 6.34−6.33 (d, 1H, J = 3.30 Hz, furylic proton); 2.39 (s, 3H). ^{13}C NMR (100 MHz, $CDCl_3$, δ): 166.60, 153.10, 144, 143.60, 130, 129.80, 128.70, 128.10, 114.90, 111.50, 111.10, 11.20. GC−MS (70 eV) m/z (rel intens): 225 (M^+, 40), 184 (14), 183 (100), 154 (17), 127 (13), 102 (12), 43 (11). Anal. Calcd for $C_{14}H_{11}NO_2$: C, 74.65; H, 4.92; N, 6.22; O, 14.21. Found: C, 74.48; H, 4.94; N, 6.19.

5-Methyl-4-phenyl-3-(tetrahydrofuran-2-yl)isoxazole (3r). 16% yield. Colorless semisolid. FT-IR (neat): 3058, 2924, 2852, 1629, 1600, 1500, 1444, 1237, 1057, 1012, 920, 771, 701 cm^{-1}. ^1H NMR (500 MHz, $CDCl_3$, δ): 7.44−7.41 (m, 2H, aromatic protons); 7.37−7.34 (m, 3H, aromatic protons); 4.97 (t, 1H, J = 6.90 Hz); 3.91−3.83 (m, 2H); 2.39 (s, 3H); 2.22−2.08 (m, 2H); 2.05−1.85 (m, 2H). ^{13}C NMR (125 MHz, $CDCl_3$, δ): 166.10, 162.60, 130, 129.70, 128.60, 127.60, 116.20, 72.70, 68.40, 30.20, 26, 11.40. GC−MS (70 eV) m/z (rel intens): 229 (M^+, 12), 186 (6), 173 (6), 158 (4), 117 (10), 115 (6), 103 (7), 89 (9), 77 (5), 71 (100), 63 (4), 51 (5), 43 (30), 41 (9). Anal. Calcd for $C_{14}H_{15}NO_2$: C, 73.34; H, 6.59; N, 6.11.

Synthesis of 3-(5-Bromofuran-2-yl)-5-methyl-4-phenylisoxazole (3s). 3-(Furan-2-yl)-5-methyl-4-phenylisoxazole (**3q**) (0.152g, 0.670 mmol) dissolved in anhydrous DMF (6 mL), contained in a round-bottom flask equipped with magnetic stirring, was cooled to 0 °C. NBS (0.144g, 0.810 mmol) was slowly added, and the obtained suspension was stirred for 2 h at room temperature. Then water was added. Ethyl acetate was added. The two phases were separated, and the aqueous layer was extracted three times with ethyl acetate. The combined organic extracts were washed with brine to remove DMF, then dried over anhydrous Na_2SO_4, and the solvent was evaporated under vacuum. Column chromatography (silica gel, petroleum ether/ethyl acetate = 9/1) of the residue affords the 3-(5-bromofuran-2-yl)-5-methyl-4-phenylisoxazole (**3s**) in 95% yield as a white solid.

3-(5-Bromofuran-2-yl)-5-methyl-4-phenylisoxazole (3s). 60% yield. Mp 91−92 °C (petroleum ether). White powder. FT-IR (KBr): 3143, 3055, 2960, 2923, 2851, 1632, 1505, 1434, 1408, 1236, 1202, 1122, 1019, 984, 921, 896, 796, 774, 721, 704, 676, 561 cm^{-1}. ^1H NMR (400 MHz, $CDCl_3$, δ): 7.44−7.35 (m, 3H, aromatic protons); 7.26−7.23 (m, 2H, aromatic protons); 6.24 (d, 1H, J = 3.30 Hz, furylic proton); 6.20 (d, 1H, J = 3.30 Hz, furylic proton); 2.34 (s, 3H). ^{13}C NMR (100 MHz, $CDCl_3$, δ): 166.70, 152.10, 145.80, 129.90, 129.30, 128.70, 128.30, 124.10, 114.60, 113.80, 112.90, 11.10. GC−MS (70 eV) m/z (rel intens): 305 [(M^+ + 2), 47], 303 (M^+, 100), 264 (13), 263 (98), 262 (23), 261 (100), 234 (10), 232 (10), 154 (54), 153 (33), 129 (12), 127 (31), 77 (9), 43 (14). Anal. Calcd for $C_{14}H_{10}BrNO_2$: C, 55.29; H, 3.31; N, 4.61. Found: C, 55.53; H, 3.67; N, 4.34.

Synthesis of (*Z*)-4-Amino-4-(5-chlorofuran-2-yl)-3-phenylbut-3-en-2-one (4) and (*Z*)-4-Amino-4-(furan-2-yl)-3-phenylbut-3-en-2-one (5).[32] A solution of 3-(5-chlorofuran-2-yl)-5-methyl-4-phenylisoxazole (0.504g, 1.946 mmol) in EtOH (10 mL) was hydrogenated over Raney Ni (1.512g) at room temperature and atmospheric pressure for 6 h in a round-bottom flask equipped with magnetic stirring. The catalyst was removed by filtration, and the solution was concentrated in vacuo. Column chromatography (silica gel, petroleum ether/ethyl acetate = 19/1) of the residue affords the (*Z*)-4-amino-4-(5-chlorofuran-2-yl)-3-phenylbut-3-en-2-one (**4**) in 71% yield and the (*Z*)-4-amino-4-(furan-2-yl)-3-phenylbut-3-en-2-one (**5**) in 28% yield.

(*Z*)-4-Amino-4-(5-chlorofuran-2-yl)-3-phenylbut-3-en-2-one (4). 71% yield. Yellow semisolid. FT-IR (KBr): 3395, 3209, 3158, 3138, 3057, 2923, 2852, 1603, 1577, 1496, 1449, 1416, 1291, 1258, 1209, 1072, 1018, 968, 941, 794, 755, 699 cm^{-1}. ^1H NMR (400 MHz, $CDCl_3$, δ): 11.20−10.20 (bs, 1H, NH exchanges with D_2O); 7.42−7.36 (m, 3H, aromatic protons); 7.25−7.20 (m, 2H, aromatic protons); 6.40−5.20 (bs, 1H, NH exchanges with D_2O); 5.94−5.93 (d, 1H, J = 3.70 Hz, furylic proton); 4.93−4.92 (d, 1H, J = 3.70 Hz, furylic proton); 1.90 (s, 3H). ^{13}C NMR (100 MHz, $CDCl_3$, δ): 198, 147.20, 146.60, 139.60, 137.90, 132.10, 129.20, 127.60, 117.80, 109, 107.50, 29.80. GC−MS (70 eV) m/z (rel intens): 263 [(M^+ + 2), 6], 261 (M^+, 17), 227 (16), 226 (100), 183 (22), 170 (7), 154 (16), 131 (6), 128 (10), 127 (15), 103 (6), 77 (6), 43 (6). Anal. Calcd for $C_{14}H_{12}NO_2Cl$: C, 64.25; H, 4.62; N, 5.35. Found: 64.54; H, 4.81; N, 5.69.

(*Z*)-4-Amino-4-(furan-2-yl)-3-phenylbut-3-en-2-one (5). 28% yield. Yellow solid. Mp 102−104 °C (hexane). FT-IR (KBr): 3488, 3214, 3145, 3124, 3049, 1610, 1588, 1569, 1493, 1457, 1414, 1373, 1286, 1263, 1222, 1029, 1014, 974, 920, 751, 700 cm^{-1}. ^1H NMR (400 MHz, $CDCl_3$, δ): 11.20−10.60 (bs, 1H, NH exchanges with D_2O); 7.38−7.33 (m, 4H, aromatic protons); 7.21−7.19 (m, 2H, aromatic protons); 6.13−6.12 (dd, 1H, J = 3.70 Hz, J = 1.50 Hz, furylic proton); 6.30−5.60 (bs, 1H, NH exchanges with D_2O); 4.97−4.96 (d, 1H, J = 3.70 Hz, furylic proton); 1.87 (s, 3H). ^{13}C NMR (100 MHz, $CDCl_3$, δ): 197.90, 147.90, 147.60, 143, 140, 132.20, 129.10, 127.40, 115.70, 112.20, 107.60, 29.90. GC−MS (70 eV) m/z (rel intens): 227 (M^+, 100), 212 (26), 210 (32), 185 (53), 184 (33), 173 (35), 156 (22), 154 (13), 139 (11), 129 (11), 128 (24), 127 (13), 115 (11), 77 (9), 43 (9). Anal. Calcd for $C_{14}H_{13}NO_2$: C, 73.99; H, 5.77; N, 6.16. Found: 74.40; H, 5.81; N, 5.99.

Synthesis of Methyl 3-(5-Chlorofuran-2-yl)-5-hydroxy-4-phenyl-4,5-dihydroisoxazole-5-carboxylate (2i).[72] A 2.5 M solution of *n*-butyllithium in hexane (0.54 mL, 1.341 mmol) was added to diisopropylamine (0.19 mL, 1.341 mmol) in THF (7 mL) at 0 °C under nitrogen atmosphere, using a nitrogen-flushed, three-neck flask equipped with a magnetic stirrer, a nitrogen inlet, and two dropping funnels. After the mixture had been stirred for 15 min, phenylpiruvic acid (100 mg, 0.6097 mmol) in THF (3 mL) was dropwise added. The red reaction mixture was stirred at 0 °C for 1 h. Then a solution of 5-chlorofuran-2-carbonitrile oxide (0.610 mmol) in THF (3 mL) was added. The reaction mixture was allowed to reach room temperature and stirred overnight and then quenched by adding aqueous NH_4Cl solution. Then HCl, 1 N, was added until the mixture was acidic, and the aqueous layer was extracted three times with $CHCl_3$. The combined organic extracts were dried over anhydrous Na_2SO_4 and then evaporated under vacuum. The residue was further purified by washing with Et_2O to afford the 3-(5-chlorofuran-2-yl)-5-hydroxy-4-phenyl-4,5-dihydroisoxazole-5-carboxylic acid (**2h**) as a white solid (188 mg), then converted into the corresponding methyl ester (**2i**). ^1H NMR (300 MHz, $CDCl_3$, δ): 11−10.75 (bs, 2H, COOH exchange with D_2O; one proton for each stereoisomer); 7.40−7.21 (m, 5H, aromatic protons, 5H for each

stereoisomer); 6.42−6.40 (d, J = 3.60 Hz, 1H, furylic proton, minor isomer); 6.15−6.13 (d, J = 3.60 Hz, 1H, furylic proton, minor isomer); 6.08−6.06 (d, J = 3.40 Hz, 1H, furylic proton, major isomer); 5.99−5.97 (d, J = 3.40 Hz, 1H, furylic proton, major isomer); 5.24 (s, 1H, major isomer); 4.76 (s, 1H, minor isomer); 3.20−3.00 (bs, 2H, OH exchange with D_2O; one proton for each stereoisomer). ^{13}C NMR (75 MHz, $CDCl_3$, δ): 171.41, 150.20, 144.51, 139.03, 133.29, 130.76, 130.49, 129.56, 129.14, 128.67, 128.41, 128.10, 105.76, 46.93. LC−MS (ESI^-): 306 [$(M-1)^-$, 39], 117 (100). A 1.3 M solution of BF_3/MeOH (0.942 mL, 1.224 mmol) was added at 0 °C to the 3-(5-chlorofuran-2-yl)-5-hydroxy-4-phenyl-4,5-dihydroisoxazole-5-carboxylic acid (**2h**) (188 mg, 0,612 mmoli). The reaction mixture was allowed to reach room temperature and then stirred for 3 h. The MeOH was evaporated under reduced pressure, and the aqueous layer was extracted three times with ethyl acetate. The combined organic extracts were dried over anhydrous Na_2SO_4, and the solvent was evaporated under reduced pressure. Column chromatography (silica gel, petroleum ether/ethyl acetate = 8/2) of the residue (172 mg) affords the methyl 3-(5-chlorofuran-2-yl)-5-hydroxy-4-phenyl-4,5-dihydroisoxazole-5-carboxylate (**2i**) in 72%yield.

Methyl 3-(5-Chlorofuran-2-yl)-5-hydroxy-4-phenyl-4,5-dihydroisoxazole-5-carboxylate (2i). 72% yield (141 mg). Yellow oil. ^1H NMR (300 MHz, $CDCl_3$, δ): 7.36−7.14 (m, 5H, aromatic protons for each stereoisomer); 6.46−6.45 (d, J = 3.20 Hz, 1H, furylic proton, minor isomer); 6.17−6.16 (d, J = 3.20 Hz, 1H, furylic proton, minor isomer); 6.10−6.09 (d, J = 3.30 Hz, 1H, furylic proton, major isomer); 6.04−6.03 (d, J = 3.30 Hz, 1H, furylic proton, major isomer); 5.21 (s, 1H, major isomer); 4.78 (s, 1H, minor isomer); 4.60−4.20 (bs, 2H, OH exchange with D_2O, 1H for each stereoisomer); 3.94 (s, 3H, OCH_3, major isomer); 3.30 (s, 3H, OCH_3, minor isomer). ^{13}C NMR (75 MHz, $CDCl_3$, δ): 168.60, 150.50, 143.20, 140, 130.80, 130.50, 129, 128.85, 128.82, 116.30, 108.80, 108.60, 103.90, 58.90, 54.40. GC−MS (70 eV) m/z (rel intens): 323 [$(M^+ + 2)$, 19], 321 (M^+, 47), 262 (16), 219 (9), 218 (10), 217 (16), 216 (20), 188 (15), 182 (12), 155 (20), 154 (100), 153 (9), 140 (10), 139 (25), 135 (62), 128 (12), 127 (25), 118 (19), 115 (11), 107 (23), 102 (17), 91 (22), 90 (23), 89 (29), 79 (22), 77 (24), 73 (12), 64 (11), 63 (15).

Synthesis of 3-(5-Chlorofuran-2-yl)-4-phenylisoxazole-5-carboxylic Acid (3h). A solution of Na_2CO_3 (237 mg, 2.24 mmol) in water (10 mL) was added to methyl [3-(5-chlorofuran-2-yl)-4-phenyl-2-isoxazolin-5-yl]carboxylate (**2i**) (360 mg, 1.12 mmol) in MeOH (10 mL) contained in a round-bottom flask equipped with magnetic stirrer. The reaction mixture was refluxed for 2 h. The MeOH was evaporated under reduced pressure, and the aqueous layer was extracted three times with $CHCl_3$. The combined organic extracts were dried over anhydrous Na_2SO_4, and the solvent was evaporated under reduced pressure. The residue was crystallized by $CHCl_3$/hexane to afford [3-(5-chlorofuran-2-yl)-4-phenylisoxazol-5-yl]carboxylic acid (**3h**) (300 mg, 92% yield).

3-(5-Chlorofuran-2-yl)-4-phenylisoxazole-5-carboxylic Acid (3h). 92% yield. White solid. Mp 168−170 °C. FT-IR (KBr): 3500−2850, 1709, 1614, 1592, 1521, 1454, 1416, 1392, 1305, 1249, 1208, 1153, 1122, 1022, 1006, 981, 941, 899, 779, 696 cm^{-1}. ^1H NMR (300 MHz, $CDCl_3$, δ): 7.48−7.42 (m, 3H, aromatic protons); 7.39−7.32 (m, 2H, aromatic protons); 7.00−6.50 (bs, 1H, OH exchanges with D_2O); 6.14 (d, J = 3.60 Hz, 1H, furyl proton); 6.12 (d, J = 3.60 Hz, 1H, furyl proton). ^{13}C NMR (75 MHz, $CDCl_3$, δ): 160.20, 155.30, 154.10, 142.10, 139.70, 129.90, 129.60, 128.80, 127.40, 124.40, 115.30, 108.40. LC−MS (ESI^-): 288 [$(M-1)^-$, 69], 117 (100). Anal. Calcd for $C_{14}H_8ClNO_4$: C, 58.05; H, 2.78; N, 4.83. Found: C, 57.65; H, 2.89; N, 4.68.

Synthesis of Methyl [3-(5-Chlorofuran-2-yl)-4-phenylisoxazol-5-yl]carboxylate (3i). To [3-(5-chlorofuran-2-yl)-4-phenylisoxazol-5-yl]carboxylic acid (**3h**) (1.119g, 3.87 mmol) in MeOH (28 mL), H_2SO_4 (14 mL) was slowly added. Then the reaction mixture was stirred for 4 h at room temperature, and soon after, H_2SO_4 (1 mL) was added. After 2 h, ethyl ether and ice were added to the reaction mixture. The two phases were separated, and the aqueous layer was washed three times with ethyl ether. The combined extracts were dried over anhydrous Na_2SO_4, and then the solvent was evaporated under reduced pressure. Column chromatography (silica gel, mobile phase of petroleum ether/ethyl acetate = 10:1) of the residue (1.044 g) afforded the product (0.52 g) with 45% yield.

Methyl [3-(5-Chlorofuran-2-yl)-4-phenylisoxazol-5-yl]-carboxylate (3i). 45% yield. White solid. Mp 130−131 °C. FT-IR (KBr): 3135, 2962, 2924, 2848, 1737, 1610, 1594, 1521, 1491, 1441, 1417, 1347, 1307, 1240, 1215, 1149, 1116, 1031, 1014, 987, 936, 803, 698 cm^{-1}. ^1H NMR (500 MHz, $CDCl_3$, δ): 7.48−7.47 (m, 3H, aromatic protons); 7.35−7.33 (m, 2H, aromatic protons); 6.14 (m, 1H, furyl proton); 6.12 (m, 1H, furyl proton); 3.86 (s, 3H, CH_3). ^{13}C NMR (75 MHz, $CDCl_3$, δ): 157.33, 155.99, 153.86, 142.34, 139.54, 130, 129.48, 128.75, 127.71, 123.33, 115.09, 108.36, 52.95. GC−MS (70 eV) m/z (rel intens): 305 [$M(^{37}Cl)^+$, 35], 303 [$M(^{35}Cl)^+$,100], 249 (12), 247 (36), 246 (21), 244 (29), 240 (21), 232 (20), 218 (13), 216 (30), 212 (49), 190 (28), 189 (14), 188 (84), 180 (17), 153 (57), 152 (51), 145 (19), 129 (25), 128 (16), 127 (29), 126 (12), 115 (10), 91 (19), 89 (96), 77 (24), 75 (16), 73 (13), 63 (27), 59 (10), 51 (11). Anal. Calcd for $C_{15}H_{10}ClNO_4$: C, 59.32; H, 3.32; N, 4.61. Found: C, 59.69; H, 3.51; N, 4.30.

Synthesis of 3-(Morpholin-1-yl)propyl [3-(5-Chlorofuran-2-yl)-4-phenylisoxazol-5-yl]carboxylate (3n). A mixture of [3-(5-chlorofuran-2-yl)-4-phenylisoxazol-5-yl]carboxylic acid (**3h**) (570 mg, 1.97 mmol) and thionyl chloride (5 mL) was kept under reflux for 2 h. Then the excess of thionyl chloride was removed under reduced pressure. To the residue solubilized in CH_2Cl_2 (5 mL) and cooled by an ice bath, NEt_3 (0.26 mL) and 4-(3-hydroxypropyl)morpholine (0.30 mL, 2.17 mmol) were added. The reaction mixture was stirred at room temperature for 2 h. Then saturated aqueous Na_2CO_3 solution was added to give alkaline pH and the product extracted with methylene chloride. The combined extracts were dried over anhydrous Na_2SO_4 and concentrated under reduced pressure. Column chromatography (silica gel, mobile phase of petroleum ether/ethyl acetate = 9:1) of the residue (702 mg) afforded the product (59 mg, 72% yield).

3-(Morpholin-1-yl)propyl [3-(5-Chlorofuran-2-yl)-4-phenylisoxazol-5-yl]carboxylate (3n). 72% yield. Mp 82.00−83.70 °C. FT-IR (KBr): 3140, 3059, 2958, 2854, 2813, 1738, 1690, 1624, 1519, 1447, 1347, 1305, 1239, 1208, 1191, 1118, 1020, 985, 941, 900, 863, 792, 700 cm^{-1}. ^1H NMR (300 MHz, $CDCl_3$, δ): 7.46−7.43 (m, 3H, aromatic protons); 7.33−7.30 (m, 2H, aromatic protons); 6.10 (d, J = 3.40 Hz, 1H, furyl proton); 6.08 (d, J = 3.40 Hz, 1H, furyl proton); 4.30−4.26 (t, J = 6.30 Hz, 2H, CH_2O); 3.69−3.63 (m, 4H, CH_2OCH_2); 2.40−2.31 (m, 4H, CH_2NCH_2); 2.19−2.15 (t, J = 7.10 Hz, 2H, CH_2N); 1.76−1.67 (m, 2H, $CH_2CH_2CH_2$). ^{13}C NMR (75 MHz, $CDCl_3$, δ): 156.89, 156.23, 153.83, 142.35, 139.46, 130.02, 129.44, 128.76, 128.05, 122.84, 115.05, 108.37, 67.06, 64.59, 55.08, 53.73, 25.49. GC−MS (70 eV) m/z (rel intens): 418 [$M(^{37}Cl)^+$, 2], 416 [$M(^{35}Cl)^+$, 4], 100 (100). Anal. Calcd for $C_{15}H_{10}ClNO_4$: C, 60.51; H, 5.08; N, 6.72. Found: C, 60.55; H, 5.10; N, 6.69. FT-IR (KBr) of 3-(morpholin-1-yl)propyl [3-(5-chlorofuran-2-yl)-4-phenylisoxazol-5-yl]carboxylate hydrochloride: 3150, 2956, 2863, 2595−2400, 1746, 1630, 1606, 1521, 1446, 1412, 1388, 1346, 1307, 1253, 1206, 1182, 1133, 1101, 1019, 981, 938, 897, 868, 798, 707 cm^{-1}.

Synthesis of 3-Bromopropyl [3-(5-Chlorofuran-2-yl)-4-phenylisoxazol-5-yl]carboxylate (3o). A mixture of [3-(5-chlorofuran-2-yl)-4-phenylisoxazol-5-yl]carboxylic acid (**3h**) (239 mg, 0.83 mmol) and thionyl chloride (2 mL) was kept under reflux for 2 h. Then the excess thionyl chloride was removed under reduced pressure. To the residue solubilized with CH_2Cl_2 (5 mL) and cooled by an ice-bath, NEt_3 (83.83 mg, 0.83 mmol) and 3-bromo-1-propanol (116 mg, 0.83 mmol) were added. The reaction mixture was stirred at room temperature for 12 h. Then saturated aqueous Na_2CO_3 solution was added to give alkaline pH and the product extracted with $CHCl_3$. The combined extracts were dried over anhydrous Na_2SO_4 and concentrated under reduced pressure. The product (235 mg) was obtained with 69% yield.

3-Bromopropyl [3-(5-Chlorofuran-2-yl)-4-phenylisoxazol-5-yl]carboxylate (3o). 69% yield. White solid. Mp 100−101 °C. FT-IR (KBr): 3136, 3076, 2963, 2924, 1737, 1623, 1605, 1519, 1448, 1463, 1424, 1413, 1385, 1345, 1310, 1249, 1209, 1184, 1152, 1019, 985, 944, 901, 884, 793, 773, 702 cm^{-1}. ^1H NMR (400 MHz, $CDCl_3$, δ): 7.49−7.45 (m, 3H, aromatic protons); 7.33−7.30 (m, 2H, aromatic protons); 6.11 (d, J = 3.60 Hz, 1H, furyl proton); 6.07 (d, J = 3.60 Hz, 1H, furyl proton); 4.34−4.32 (t, J = 6.10 Hz, 2H, $COOCH_2$); 3.07−3.04 (t, J =

dx.doi.org/10.1021/jm301905a | J. Med. Chem. 2013, 56, 4277−4299

6.10 Hz, 2H, CH_2Br); 2.06−2.00 (quintet, J = 6.10 Hz, 2H, $CH_2CH_2CH_2$). ^{13}C NMR (100 MHz, $CDCl_3$, δ): 156.66, 156.01, 153.85, 142.25, 139.58, 129.89, 129.55, 128.86, 128.04, 123, 115.11, 108.38, 63.77, 31.35, 28.99. GC−MS (70 eV) m/z (rel intens): 411 [$(M^+ + 2)$, 18], 409 (M^+, 18), 282 (10), 281 (12), 244 (10), 207 (11), 188 (12), 153 (13), 152 (22), 145 (100), 118 (32), 89 (36), 73 (16), 63 (11), 44 (12), 41 (12). Anal. Calcd for $C_{17}H_{13}BrClNO_4$: C, 49.72; H, 3.17; N, 3.41. Found: C, 49.70; H, 3.15; N, 3.39.

Synthesis of 3-(Nitroxy)propyl [3-(5-Chlorofuran-2-yl)-4-phenylisoxazol-5-yl]carboxylate (3p). To 3-bromopropyl [3-(chlorofuran-2-yl)-4-phenylisoxazol-5-yl]carboxylate (**3o**) (200 mg, 0.49 mmol) in CH_3CN (1 mL), small aliquots of $AgNO_3$ (92 mg) were added. The reaction mixture was stirred at room temperature for 12 h, and then further small aliquots of $AgNO_3$ (92 mg) were added. After 10 h, AgBr was filtered off, and then the CH_3CN used as reaction solvent to wash AgBr was combined and distilled under reduced pressure. Column chromatography (silica gel, mobile phase of petroleum ether/ethyl acetate = 9:1) of the residue (180 mg) afforded the product (145 mg) with 90% yield.

3-(Nitroxy)propyl [3-(5-Chlorofuran-2-yl)-4-phenylisoxazol-5-yl]carboxylate (3p). 90% yield. Mp 79.00−79.80 °C. FT-IR (neat): 3144, 3055, 2925, 2853, 1740, 1631, 1518, 1447, 1414, 1346, 1306, 1280, 1209, 1188, 1156, 1021, 863, 700 cm^{-1}. ^1H NMR (300 MHz, $CDCl_3$, δ): 7.52−7−45 (m, 3H, aromatic protons); 7.37−7−30 (m, 2H, aromatic protons); 6.13 (d, J = 3.40 Hz, 1H, furyl proton); 6.10 (d, J = 3.40 Hz, 1H, furyl proton); 4.34−4.30 (t, J = 6.20 Hz, 2H, $COOCH_2$); 4.18−4.14 (t, J = 6.20 Hz, 2H, CH_2ONO_2); 2.00−1.92 (quintet, J = 6.20 Hz, 2H, $CH_2CH_2CH_2$). ^{13}C NMR (75 MHz, $CDCl_3$, δ): 156.55, 155.85, 153.89, 142.21, 139.65, 129.89, 129.59, 128.87, 128.04, 123.17, 115.17, 108.41, 69.17, 61.84, 26.16. GC−MS (70 eV) m/z (rel intens): 331 [$(M(^{37}Cl)^+ - 63$, 37], 329 [$M(^{35}Cl)^+ - 63$, 100], 315 (31), 244 (37), 216 (17), 207 (11), 188 (27), 153 (23), 145 (16), 128 (11), 127 (12), 89 (37), 86 (20), 63 (10), 51 (11), 43 (36), 41 (14). Anal. Calcd for $C_{17}H_{13}ClN_2O_7$: C, 51.99; H, 3.34; N, 7.13. Found: C, 52.00; H, 3.35; N, 7.19.

Synthesis of 3-(5-Chlorofuran-2-yl)-5-hydroxymethyl-4-phenylisoxazole (3l).[72] A 2 M solution in THF of borane−methyl sulfide complex (BMS) (1.72 mL, 3.44 mmol) was dropwise added to [3-(5-chlorofuran-2-yl)-4-phenylisoxazol-5-yl]carboxylic acid (**3h**) (500 mg, 1.73 mmol) in anhydrous THF (6 mL) kept at 0 °C, under stirring and nitrogen atmosphere. The reaction mixture was allowed to warm to room temperature, and after 5 h, additional BMS (1.72 mL) was added. After a further 5 h the reaction was stopped by adding H_2O (10 mL), 3 N NaOH (10 mL), and H_2O_2 (30% w/w, 10 mL).The obtained mixture was stirred for 30 min. The two phases were separated, and the aqueous layer was washed three times with EtOAc. The combined organic extracts were dried over anhydrous Na_2SO_4, and the solvent was removed under reduced pressure. Column chromatography (silica gel, mobile phase of petroleum ether/ethyl acetate = 9:1 to 1:1, gradually modified as soon as a single substance was eluted) of the residue (470 mg) afforded the product that was recrystallized (248 mg, 52% yield) from hexane/EtOAc.

3-(5-Chlorofuran-2-yl)-5-hydroxymethyl-4-phenylisoxazole (3l). 52% yield. Mp 102−103 °C. FT-IR (KBr): 3600−3210, 3144, 3128, 3054, 2927, 1594, 1511, 1447, 1405, 1356, 1289, 1216, 1129, 1019, 1010, 942, 925, 902, 802, 769, 702 cm^{-1}. ^1H NMR (400 MHz, $CDCl_3$, δ): 7.45−7.41 (m, 3H, aromatic protons); 7.35−7.30 (m, 2H, aromatic protons); 6.28 (d, J = 3.4 Hz, 1H, furyl proton); 6.12 (d, J = 3.4 Hz, 1H, furyl proton); 4.65 (s, 2H, CH_2OH); 2.30−2.05 (bs, 1H, OH exchanges with D_2O). ^{13}C NMR (100 MHz, $CDCl_3$, δ): 167.61, 152.55, 143.22, 138.95, 130.21, 129.07, 129.01, 128.49, 116.57, 114.31, 108.23, 54.80. GC−MS (70 eV) m/z (rel intens): 277 [$M(^{37}Cl)^+$, 33], 275 [$M(^{35}Cl)^+$, 100], 246 (12), 244 (32), 238 (14), 218 (14), 217 (16), 216 (32), 212 (29), 211 (31), 190 (21), 188 (58), 183 (10), 182 (11), 180 (10), 154 (42), 153 (38), 152 (35), 129 (18), 128 (14), 127 (25), 91 (14), 89 (42), 77 (13), 63 (11). Anal. Calcd for $C_{14}H_{10}ClNO_3$: C, 60.99; H, 3.66; N, 5.08. Found: C, 61.00; H, 3.62; N, 5.06.

Synthesis of 5-Acetoxymethyl-3-(5-chlorofuran-2-yl)-4-phenylisoxazole (3m). To a solution of 3-(5-chlorofuran-2-yl)-5-hydroxymethyl-4-phenylisoxazole (**3l**) (350 mg, 1.273 mmol) and Ac_2O (5.2 mL) kept under stirring and at 0 °C, Et_3N (0.213 mL, 1.553 mmol) was added. The reaction mixture was allowed to reach room temperature and stirred for 1.5 h. Then ice and saturated aqueous $NaHCO_3$ solution (10 mL) were added. The two phases were separated, and the aqueous layer was extracted three times with CH_2Cl_2. The combined organic extracts were dried over anhydrous Na_2SO_4 with the solvent under reduced pressure. Column chromatography (silica gel, mobile phase of petroleum ether/ethyl acetate = 9:1 and 8:2 after the elution of the first substance) of the residue afforded the product with 60% yield.

5-Acetoxymethyl-3-(5-chlorofuran-2-yl)-4-phenylisoxazole (3m). 60% yield. FT-IR (neat): 3132, 3053, 2921, 1751, 1636, 1517, 1432, 1412, 1372, 1359, 1226, 1127, 1048, 1018, 985, 939, 903, 790, 777, 704 cm^{-1}. ^1H NMR (400 MHz, $CDCl_3$, δ): 7.44−7.42 (m, 3H, aromatic protons); 7.30−7.28 (m, 2H, aromatic protons); 6.24 (d, J = 3.60 Hz, 1H, furyl proton); 6.11 (d, J = 3.60 Hz, 1H, furyl proton); 5.07 (s, 2H, CH_2); 2.02 (s, 3H, CH_3). ^{13}C NMR (75 MHz, $CDCl_3$, δ): 170.29, 163.47, 152.66, 143.06, 139.05, 130.17, 129.18, 129.08, 128.14, 118.14, 114.40, 108.25, 55.38, 20.73. GC−MS (70 eV) m/z (rel intens): 319 [$M(^{37}Cl)^+$, 33], 317 [$M(^{35}Cl)^+$, 90], 277 (18), 276 (10), 275 (49), 240 (18), 238 (10), 217 (23), 216 (11), 213 (17), 212 (100), 211 (32), 190 (11), 188 (27), 182 (11), 154 (20), 153 (26), 152 (21), 129 (15), 127 (19), 91 (12), 89 (26), 73 (11), 43 (30). Anal. Calcd for $C_{16}H_{12}ClNO_3$: C, 64.48; H, 3.81; N, 4.41. Found: C, 64.46; H, 3.82; N, 4.46.

Synthesis of Methyl [3-Aryl-5-phenylisoxazol-4-yl]-carboxylates (3t, 3u). Freshly prepared arylnitrile oxide (0.99 mmol) was added to a stirred methyl 3-phenylpropiolate (Scheme 7) (159 mg, 0.99 mmol) in anhydrous CH_2Cl_2 (5 mL) kept at room temperature and under nitrogen atmosphere. The reaction mixture was stirred at room temperature for 72 h, and then H_2O was added. The two phases were separated, and the aqueous layer was extracted three times with CH_2Cl_2. The combined organic phases were dried over anhydrous Na_2SO_4, and then the solvent was evaporated under reduced pressure. Column chromatography (silica gel, mobile phase of petroleum ether/ethyl acetate = 10:1) of the residue afforded the product.

Methyl [3-(5-Chlorofuran-2-yl)-5-phenylisoxazol-4-yl]-carboxylate (3t). 54% yield (162 mg). Mp 113−117 °C (dec 86.4 °C). FT-IR (KBr): 3113, 3050, 2924, 2853, 1723, 1610, 1515, 1491, 1444, 1430, 1346, 1314, 1235, 1210, 1128, 1050, 1019, 937, 805, 776, 687 cm^{-1}. ^1H NMR (300 MHz, $CDCl_3$, δ): 7.84−7.80 (m, 2H, aromatic protons); 7.57−7.47 (m, 3H, aromatic protons); 7.22 (d, J = 3.60 Hz, 1H, furyl proton); 6.34 (d, J = 3.60 Hz, 1H, furyl proton 3.84 (s, 3H, CH_3). ^{13}C NMR (75 MHz, $CDCl_3$, δ): 173.01, 162.45, 153.29, 142.22, 139.32, 131.70, 128.93, 128.82, 126.68, 116.31, 108.58, 106.91, 52.46. GC−MS (70 eV) m/z (rel intens): 305 [$(M(^{37}Cl)^+$, 13], 303 [$M(^{35}Cl)^+$, 39], 240 (5), 105 (100), 77 (38), 51 (7). Anal. Calcd for $C_{15}H_{10}ClNO_4$: C, 59.32; H, 3.32; N, 4.61. Found: C, 59.31; H, 3.30; N, 4.60.

Methyl [3,5-Diphenylisoxazol-4-yl]carboxylate (3u). 67% yield. Mp 102.50−104.80 °C. FT-IR (KBr): 3062, 2958, 1729, 1610, 1593, 1573, 1494, 1448, 1408, 1320, 1237, 1188, 1120, 1076, 1043, 941, 806, 768, 726, 697 cm^{-1}. ^1H NMR (300 MHz, $CDCl_3$, δ): 7.96−7.88 (m, 2H, aromatic protons); 7.70−7.63 (m, 2H, aromatic protons); 7.56−7.46 (m, 6H, aromatic protons); 3.72 (s, 3H, CH_3). ^{13}C NMR (75 MHz, $CDCl_3$, δ): 172.73, 163.25, 163.11, 131.56, 130.16, 129.14, 128.92, 128.83, 128.74, 128.57, 127.07, 108.24, 52.25. GC−MS (70 eV) m/z (rel intens): 279 (M^+, 79), 278 (17), 251 (6), 220 (5), 202 (7), 143 (10), 105 (100), 77 (47), 51 (9). Anal. Calcd for $C_{17}H_{13}NO_3$: C, 73.11; H, 4.69; N, 5.02. Found: C, 73.06; H, 4.67; N, 5.06.

Synthesis of 3-Aryl-5-phenylisoxazol-4-yl carboxylic Acid (3v, 3w). KOH (30 mg, 0.475 mmol) in H_2O (2.5 mL) was added to methyl 3-aryl-5-phenylisoxazol-4-yl]carboxylate (**3t−u**) (72 mg, 0.238 mmol) in THF (3 mL). The reaction mixture was stirred overnight at room temperature. Then THF was distilled under reduced pressure and ethyl ether was added to the residue. The two phases were separated. 10% HCl was added to the aqueous phase till pH < 5, and the product was extracted three times with ethyl ether. The combined organic phases were dried over anhydrous Na_2SO_4, and then the solvent was evaporated under reduced pressure. The residue recrystallized from $CHCl_3$/hexane afforded the pure products as white needles.

[3-(5-Chlorofuran-2-yl)-5-phenylisoxazol-4-yl]carboxylic Acid (3v). 58% yield (40 mg). ^{1}H NMR (300 MHz, $CDCl_3$, δ): 7.87−7.84 (m, 2H, aromatic protons); 7.60−7.49 (m, 3H, aromatic protons); 7.30 (d, J = 3.6 Hz, 1H, furyl proton); 7.20−7 (bs, 1H, COOH exchange with D_2O); 6.34 (d, J = 3.60 Hz, 1H, furyl proton). ^{13}C NMR (75 MHz, $CDCl_3$, δ): 174.99, 166.21, 153.53, 141.80, 139.60, 131.98, 129.49, 128.80, 126.42, 117.30, 108.65, 106.05. Anal. Calcd for $C_{14}H_8ClNO_4$: C, 58.05; H, 2.78; N, 4.83. Found: C, 58.01; H, 2.81; N, 4.85.

(3,5-Diphenylisoxazol-4-yl)carboxylic Acid (3w). 87% yield (148 mg). FT-IR (KBr): 3600−2800, 1738, 1586, 1567, 1492, 1448, 1417, 1283, 1229, 1119, 756, 730, 692 cm^{-1}. ^{1}H NMR (500 MHz, acetone-d_6, δ): 8.00−7.98 (m, 2H, aromatic protons); 7.75−7.73 (m, 2H, aromatic protons); 7.66−7.32 (m, 7H, six aromatic protons and the proton of COOH that exchanges with D_2O). ^{13}C NMR (75 MHz, acetone-d_6, δ): 172.04, 163.10, 162.83, 131.48, 130.04, 129.11, 129.08, 128.89, 128.77, 128.52, 127.27, 108.78. GC−MS (70 eV) m/z (rel intens): 221 ($M^+ - 44$, 55), 146 (13), 144 (25), 142 (15), 133 (10), 132 (33), 105 (100), 103 (11), 91 (17), 89 (22), 77 (39), 50 (19), 44 (28), 41 (19). Anal. Calcd for $C_{16}H_{11}NO_3$: C, 72.44; H, 4.18; N, 5.28. Found: C, 72.46; H, 4.17; N, 5.30.

Human Whole Blood Assays. Subjects. Ten healthy volunteers (six females and four males between 26 and 35 years of age) were enrolled to participate in the study after its approval by the ethical committee of the University "G. D'Annunzio" in Chieti, Italy. Informed consent was obtained from each subject. The same healthy volunteers, who had not taken NSAIDs for previous 14 days, were studied on different occasions.

Effects of Diarylisoxazole Derivatives on Whole Blood COX-2 and COX-1 Activities. Novel compounds (0.0005−500 mM) were dissolved in DMSO, and 2 μL aliquots of the solutions or vehicle were pipetted directly into test tubes to give final concentrations of 0.001−1000 μM in blood. Then 1 mL aliquots of heparinized whole blood (from healthy subjects pretreated in vivo with 300 mg of aspirin 48 h before blood collection to inhibit the contribution of platelet COX-1) were added and incubated with LPS [derived from *Escherichia coli* 026:B6, final concentration of 10 μg/mL, Sigma Chemical Company (St. Louis, MO, U.S.)] for 24 h at 37 °C. PGE_2 was measured as an index of LPS-induced monocyte COX-2 activity.[33] The same concentrations of novel compounds were incubated with 1 mL of whole blood samples (collected from the same subjects in aspirin-free periods), and then they were allowed to clot at 37 °C for 1 h. Then TXB_2 production was measured as a reflection of maximally stimulated platelet COX-1 activity in response to endogenously formed thrombin.[34] Whole blood PGE_2 and TXB_2 concentrations were measured by previously described and validated radioimmunoassays (RIAs).[33,34]

Human Plasma Protein Binding. The binding of **3d**, **3g**, **3s**, and **6** to human plasma proteins was evaluated by using the TRANSIL XL PPB binding kit (Sovicell, Leipzig, Germany) by following the manufacturer's instructions. The principle of the assay is to assess the affinity of test compounds to the human plasma proteins HSA and AGP mixed in each well at a physiological ratio of 24:1. Plasma protein binding is determined by incubating 15 μL of a 32× stock solutions in 32% DMSO of test compounds with varying concentrations of the plasma proteins immobilized on silica beads. The free compound concentration was assessed by HPLC, performed by using a 1260 Infinity liquid chromatograph (Agilent Technologies) equipped with a diode array detector 1260 DAD VL+. The column was a Poroshell 120 EC-C18 (3.0 mm × 50 mm, particle size 2.70 μm). The selected wavelength was 280 nm. The mobile phase used in the separation consisted of acetonitrile and water [70/30]. The flow rate was 0.5 mL/min with an injection volume of 100 μL. All reagents and solvents were analytical grade. Retention times were 2.84 min for **3d**, 1.74 min for **3g**, 2.04 min for **3s**, and 1.99 min for **6**. The HPLC detection limit was 0.10 μM.

Effects of Diarylisoxazole Derivatives on Platelet Aggregation and TXB_2 Generation in PRP. Selected compounds (**3s**, **3g**, **3d**, **3m**, and **6**) (0.50−50 mM) were dissolved in DMSO to obtain final concentrations of 1−100 μM in PRP. Then 1 μL aliquots of the solutions or vehicle were preincubated at 37 °C for 5 min with 450 μL of PRP. Then an amount of 50 μL of AA (at a final concentration of 1 mM, from Sigma Chemical Company) or collagen [at a final concentration of 2 μg/mL, from Mascia Brunelli (Milan, Italy)] was added and platelet aggregation was followed for 5 min using a dual channel platelet aggregometer (Chrono-Log 490, Mascia Brunelli, Milan Italy), as previously described by Pedersen and FitzGerald (1985).[73] PRP samples were immediately centrifuged (3000 rpm) at 4 °C for 10 min, and plasma TXB_2 levels were assessed by RIA.

Effects of AA Concentrations on Platelet COX-1 Inhibition by Diarylisoxazole Derivatives in Washed Human Platelets. We compared the IC_{50} values of sigmoidal concentration−response curves of **3s**, **3g**, **3d**, **3m**, and **6** to affect TXB_2 generation by isolated platelets in the presence of low and high concentrations of AA (0.50 or 10 μM). These effects were compared with those of ibuprofen, indomethacin, and aspirin which inhibit COX-1 activity by three different mechanisms: simple reversible inhibition, time-dependent/slowly reversible inhibition (due to tight binding), and irreversible inhibition (due to covalent modification of COX-1, i.e., acetylation at serine 529). Fresh peripheral blood was collected with a syringe containing 10% (v/v) anticoagulant solution (65 mmol/L citric acid/85 mmol/L sodium citrate/2% glucose, pH 7.40). Washed platelets were prepared as previously described.[74] Then platelets, 200 μL at 10^8 cells/mL [in Hanks' balanced salt solution (HBSS) supplemented with 25 mM Hepes (HHBSS)/ 10% anticoagulant], were incubated with increasing concentrations of compounds (diluted from 400-fold concentrated solutions in DMSO or for aspirin 95% HBSS, 5% DMSO) for 30 min at 37 °C. Then 0.50 or 10 μM AA (Sigma Chemical Co., St. Louis, MO) was added for an additional 30 min at 37 °C.[21] After centrifugation (760g for 10 min at 4 °C), TXB_2 levels were measured in the supernatant by a specific RIA.

Assessment of COX-1 Inhibition and Its Reversibility by Diarylisoxazole Derivatives in THP-1 Cells. We studied the mechanism of inhibition of COX-1 by selected diarylisoxazole derivatives (**3s**, **3g**, **3d**, **3m**, and **6**), ibuprofen, indomethacin, and aspirin in THP-1 cells, selectively expressing COX-1 (Figure 6A). The THP-1 cell line was purchased from American Type Culture Collection (LGC Promochem, Milan, Italy) and cultured in RPMI-1640 containing 10% of fetal bovine serum (FBS), 1% penicillin/streptomycin, and L-glutamine, 2 mM. Before each experiment, 1×10^6 cells were cultured in 1 mL of RPMI-1640 supplemented with 0.50% of FBS for 16 h. First, we studied the inhibition of COX-1 activity by preincubating THP-1 cells (cultured in suspension) with the compounds at 100 μM for 30 min (at room temperature), and then AA, 20 μM, was added. They were incubated for 30 min (at 37 °C). The COX reaction was stopped by centrifugation of cell incubation at 3000 rpm for 10 min at 4 °C, and the supernatants were collected and stored at −70 °C until assayed for TXB_2 by RIA.[34] The reversibility of the interaction between COX-1 and the different compounds was evaluated by assessing the recovery of COX-1 activity after washing twice, with 10 mL of RPMI-1640, the cells previously incubated with 100 μM of the different compounds for 30 min (at room temperature). Then THP-1 cells were resuspended in RPMI-1670 and incubated with AA, 20 μM, for 30 min at 37 °C and finally centrifuged at 3000 rpm for 10 min at 4 °C and the supernatants were collected and stored at −70 °C until assayed for TXB_2 by RIA.[34] TXB_2 levels were normalized for protein content in cell lysates, which was evaluated using the Bradford method, according to manufacturer instructions (Biorad Laboratories, Milan, Italy).

Assessment of the Inhibition of COX-2 and Its Reversibility by Diarylisoxazole Derivatives in MDA-MB231 Cells. We studied the mechanism of inhibition of COX-2 by selected diarylisoxazole derivatives (**3s**, **3g**, **3d**, **3m**, and **6**), in comparison to aspirin, indomethacin, and ibuprofen, in MDA-MB231 cells, selectively expressing only COX-2 (Figure 7A). MDA-MB231 was purchased from ATCC and cultured in DMEM at high glucose containing 10% of FBS, 1% penicillin/streptomycin, and L-glutamine, 2 mM. Before each experiment, cells were plated at the concentration of 1×10^6 in 5 cm plates (volume 3 mL) containing 2 mL of DMEM supplemented with 0.50% of FBS for 16 h. First, we assessed the inhibition of COX-2 activity by preincubating the cells with vehicle (DMSO) or with the different test compounds at a final concentration of 100 μM for 30 min (at room temperature) and then stimulating with AA, 0.50 μM, for further a 30 min (at 37 °C).

The reversibility of the interaction between COX-2 and the different compounds was evaluated by assessing the recovery of COX-2 activity by washing the adhesive cells, previously preincubated with 100 μM of the different compounds. To this aim, cells were washed six times with 3 mL of DMEM and then resuspended with medium (without FBS) and stimulated with AA, 0.50 μM, for 30 min at 37 °C. In both experimental conditions (without or with washing passages), PGE_2 production was determined in medium by RIA, as an index of COX-2 activity. After trypsinization and centrifugation, protein quantification was performed by using the Bradford method.

Western Blot Analysis of COX-1 and COX-2 in THP-1 Human Monocytic Leukemia Cell Line and the MDA-MB-231 Breast Cancer Cell Line. Western blot analyses of COX-1 and COX-2, in cell lysates of THP-1 and MDA-MB-231 cells, were performed as previously described.[75] In brief, cells were lysed in Triton, 1%, with PMSF, 1 mM, and an amount of 50 μg of total proteins was loaded onto 4−9% sodium dodecyl sulfate−polyacrylamide gel electrophoresis (SDS−PAGE). Separated proteins were transferred to PVDF membranes [Bio-Rad Laboratories Inc. (CA, U.S.)] and incubated with anti-COX-1 (1:1000, rabbit polyclonal, Cayman Chemical, U.S.), anti COX-2 (1:1000, rabbit polyclonal, kindly gift from Merck), and anti-β-actin (1:2000, goat policlonal, Santa Cruz, CA, U.S.) overnight at 4 °C. Then the membranes were washed in TBS-Tween-20 and incubated with the secondary antibodies. Detection of bands was performed with ECL Plus, according to the manufacturer's instructions (GE Healthcare, Milan, Italy).

In Vivo Study. Specific pathogen-free female C57BL/6 mice, 9−11 weeks old and weighing 18−20 g, were purchased from Charles River Laboratories (Calco, LC, Italy), and all experiments were conducted in conformity with the institutional guidelines that are in compliance with national (D.L. No. 116, G.U., Suppl. 40, February 18, 1992) and international laws and policies. The study was approved by the Institutional Animal Use and Care Committee ("G.d'Annunzio" University, Chieti, Italy). All efforts were made to minimize animal suffering and to reduce the number of animals used. The animals were housed in cages up to five mice each and acclimated for 1 week under conditions of controlled temperature (20 ± 2 °C), humidity (55 ± 10%), and lighting (7:00 a.m. to 7:00 p.m.). Diet and water were supplied ad libitum during acclimatization and experimental sessions. **3d** (20 mg kg^{-1} day^{-1}, po) was dissolved in 1% carboxymethylcellulose (CMC) solution (Sigma Aldrich, Milan, Italy) and administered for 3 consecutive days to four mice. Another group of mice (n = 4) received CMC, as control group. Twenty-four hour urine collections were performed after the third dose of **3d** or CMC in order to evaluate the urinary excretion of 11-dehydro-TXB_2 (an enzymatic metabolite of TXB_2, an index of systemic TXA_2 biosynthesis in vivo, mainly platelet COX-1-derived) and 6-keto-$PGF_{1\alpha}$ (the hydrolysis product of PGI_2, which represents an index of renal biosynthesis of PGI_2, mainly of COX-2-dependent source).[36,45] 11-Dehydro-TXB_2 and 6-keto-$PGF_{1\alpha}$ levels were measured by previously validated methods, and their levels were corrected for urinary creatinine.[36,76]

Statistical Analysis. Results are expressed as the mean ± SEM. Values of $P < 0.05$ were considered statistically significant. In LPS-stimulated whole blood experiments, PGE_2 values were subtracted from their content detected in vehicle (DMSO) samples (without LPS). The effects of the test compounds, in the different experimental conditions, were reported as % inhibition of values assessed in the presence of only DMSO vehicle (without the compounds). Statistical analysis was performed with Student's t test or one-way ANOVA followed by Newman−Keuls multiple comparison test, using Instat (version 3.0 for Windows) (GraphPad, San Diego, CA). Concentration−response curves were fitted (using PRISM, GraphPad, version 5.0 for Windows), and IC_{50} values were calculated. The IC_{50} values were reported as mean values with 95% confidence intervals (CI).

Computational Chemistry. Molecular modeling and graphics manipulations were performed using the molecular operating environment (MOE; Chemical Computing Group, Montreal, Canada) and UCSF-CHIMERA (http://www.cgl.ucsf.edu/chimera)[77] software packages, running on a Linux workstation with an Intel Core i7 920 CPU and 12 GB of RAM. Figures were generated using Pymol 1.0.[78]

Ligand and Receptor Preparation. Model building and geometry optimizations of compounds **3m** and **3s** were accomplished with the MMFF94X force field, available within MOE. The crystal structure of ovine COX-1 in complex with celecoxib (PDB code 3kk6)[47] was used in the docking experiments, knowing that a comparison of the ovine and human sequences revealed a 95% sequence identity. Bound ligands and water molecules were removed. A correct atom assignment for Asn, Gln, and His residues was done, and hydrogen atoms were added using standard MOE geometries. Partial atomic charges were computed by MOE using the Amber99 force field. All heavy atoms were then fixed, and hydrogen atoms were minimized using the AMBER99 force field and a dielectric constant of 1, terminating at a gradient of 0.001 kcal mol^{-1} $Å^{-1}$.

Docking Simulations. Docking of **3m** and **3s** to COX-1 was performed with GOLD, version 5.0.1, which uses a genetic algorithm for determining the docking modes of ligands and proteins.[48] The coordinates of the cocrystallized ligand celecoxib were chosen as active-site origin. The active-site radius was set equal to 8 Å. The mobility of R120, Y355, and S530 side chains was set up using the flexible side chains option in the GOLD front end, which incorporates the Lovell rotamer library.[79] As suggested by the GOLD authors,[48] genetic algorithm default parameters were set as follows: the population size was 100; the selection pressure was 1.10; the number of operations was 105; the number of islands was 5; the niche size was 2; migrate was 10; mutate was 95; crossover was 95. A total of 200 poses were generated by GOLD and then clusterized by means of AClAP, version 1.0.[44] Briefly, AClAP is a newly developed clustering protocol implemented in a MATLAB metalanguage program, which combines a hierarchical agglomerative cluster analysis with a clusterability assessment method and a user-independent cutting rule.[49] The binding pose of compounds **3s** and **3m** is a low-energy conformation representative of the most populated cluster that, according to the Chauvenet criterion,[49] was statistically populated. Notably, such poses are also low energy docking poses according to the GOLD scoring function.

■ ASSOCIATED CONTENT

Supporting Information

Concentration−response curves for the inhibition of whole blood COX-1 and COX-2 activities by diarylisoxazole derivatives of **6**. This material is available free of charge via the Internet at http://pubs.acs.org.

■ AUTHOR INFORMATION

Corresponding Author

*For A.S.: phone, +39 080 5442753; fax, +39 080 5442724, e-mail, antonio.scilimati@uniba.it. For A.L.: phone, +39 081 678613; fax, +39 081 678012; e-mail, lavecchi@unina.it. For P.P.: phone, +39-0871- 541473; fax, +39-0871-541300; e-mail, ppatrignani@unich.it.

Author Contributions

#P.V., S.T., and M.G.P. contributed equally.

Notes

The authors declare no competing financial interest.

■ ACKNOWLEDGMENTS

We thank Istituto di Chimica dei Composti OrganoMetallici (ICCOM-CNR), Bari, Italy, and Laboratorio di Ricerca per la Diagnostica dei Beni Culturali (University of Bari, Italy) for NMR facilities, and Paola Anzellotti, Ph.D., for her eager and expert technical assistance. This work was financially supported by the PRIN (Progetti di Ricerca di Interesse Nazionale) Grants 2006065317_001/2006069143_002 (to P.P. and A.S.) and 20097FJHPZ 001 (to A.S.) from Italian Ministry of University and Research (MIUR).

■ ABBREVIATIONS USED

AGP, α_1-acid glycoprotein; AA, arachidonic acid; CMC, carboxymethylcellulose; CV, cardiovascular; CI, confidence interval; COX, cyclooxygenase; TX-M, 11-dehydro-TXB_2; FBS, fetal bovine serum; GI, gastrointestinal; HBSS, Hanks' balanced salt solution; HSA, human serum albumin; PRP, platelet rich plasma; PGI_2, prostacyclin; PG, prostaglandin; RIA, radioimmunoassay; SAR, structure−activity relationship; THF, tetrahydrofuran; TLC, thin-layer chromatography; TX, thromboxane; t, traditional; NSAID, nonsteroidal anti-inflammatory drug; UGIB, upper gastrointestinal bleeding

■ REFERENCES

(1) Smith, E. M.; Grosser, T.; Wang, M.; Yu, Y.; FitzGerald, G. A. Prostanoids in health and disease. *J. Lipid Res.* **2009**, *50*, S423−428.

(2) Rocca, B.; Spain, L. M.; Puré, E.; Langenbach, R.; Patrono, C.; FitzGerald, G. A. Distinct roles of prostaglandin H synthases 1 and 2 in T-cell development. *J. Clin. Invest.* **1999**, *103*, 1469−1477.

(3) Simmons, D. L.; Botting, R. M.; Hla, T. Cyclooxygenase isozymes: the biology of prostaglandin synthesis and inhibition. *Pharmacol. Rev.* **2004**, *56*, 387−437.

(4) Patrono, C.; Patrignani, P.; García Rodríguez, L. A. Cyclooxygenase-selective inhibition of prostanoid formation: transducing biochemical selectivity into clinical read-outs. *J. Clin. Invest.* **2001**, *108*, 7−13.

(5) Belton, O. A.; Duffy, A.; Toomey, S.; Fitzgerald, D. J. Cyclooxygenase isoforms and platelet vessel wall interactions in the apolipoprotein E knockout mouse model of atherosclerosis. *Circulation* **2003**, *108*, 3017−2303.

(6) Praticò, D.; Tillmann, C.; Zhang, Z. B.; Li, H.; FitzGerald, G. A. Acceleration of atherogenesis by COX-1-dependent prostanoid formation in low density lipoprotein receptor knockout mice. *Proc. Natl. Acad. Sci. U.S.A.* **2001**, *98*, 3358−3363.

(7) McClelland, S.; Gawaz, M.; Kennerknecht, E.; Konrad, C. S.; Sauer, S.; Schuerzinger, K.; Massberg, S.; Fitzgerald, D. J.; Belton, O. Contribution of cyclooxygenase-1 to thromboxane formation, platelet-vessel wall interactions and atherosclerosis in the ApoE null mouse. *Atherosclerosis* **2009**, *202*, 84−91.

(8) Chulada, P. C.; Thompson, M. B.; Mahler, J. F.; Doyle, C. M.; Gaul, B. W.; Lee, C.; Tiano, H. F.; Morham, S. G.; Smithies, O.; Langenbach, R. Genetic disruption of Ptgs-1, as well as Ptgs-2, reduces intestinal tumorigenesis in Min mice. *Cancer Res.* **2000**, *60*, 4705−4708.

(9) Daikoku, T.; Wang, D.; Tranguch, S.; Morrow, J. D.; Orsulic, S.; DuBoi,s, R. N.; Dey, S. K. Cyclooxygenase-1 is a potential target for prevention and treatment of ovarian epithelial cancer. *Cancer Res.* **2005**, *65*, 3735−3744.

(10) Perrone, M. G.; Scilimati, A.; Simone, L.; Vitale, P. Selective COX-1 inhibition: a therapeutic target to be reconsidered. *Curr. Med. Chem.* **2010**, *17*, 3769−3805.

(11) Patrono, C.; García Rodríguez, L. A.; Landolfi, R.; Baigent, C. Low-dose aspirin for the prevention of atherothrombosis. *N. Engl. J. Med.* **2005**, *353*, 2373−2383.

(12) Patrono, C.; Baigent, C.; Hirsh, J.; Roth, G. American College of Chest Physicians. Antiplatelet drugs: American College of Chest Physicians evidence-based clinical practice guidelines (8th edition). *Chest* **2008**, *133*, 199S−233S.

(13) Patrignani, P.; Filabozzi, P.; Patrono, C. Selective cumulative inhibition of platelet thromboxane production by low-dose aspirin in healthy subjects. *J. Clin. Invest.* **1982**, *69*, 1366−1372.

(14) Reilly, I. A.; FitzGerald, G. A. Inhibition of thromboxane formation in vivo and ex vivo: implications for therapy with platelet inhibitory drugs. *Blood* **1987**, *69*, 180−186.

(15) Minuz, P.; Fumagalli, L.; Gaino, S.; Tommasoli, R. M.; Degan, M.; Cavallini, C.; Lecchi, A.; Cattaneo, M.; Lechi Santonastaso, C.; Berton, G. Rapid stimulation of tyrosine phosphorylation signals downstream of G protein-coupled receptors for thromboxane A2 in human platelets. *Biochem. J.* **2006**, *400*, 127−134.

(16) Vinik, A. I.; Erbas, T.; Park, T. S.; Nolan, R.; Pittenger, G. L. Platelet dysfunction in type 2 diabetes. *Diabetes Care* **2001**, *24*, 1476−1485.

(17) Evangelista, V.; Manarini, S.; Di Santo, A.; Capone, M. L.; Ricciotti, E.; Di Francesco, L.; Tacconelli, S.; Sacchetti, A.; D'Angelo, S.; Scilimati, A.; Sciulli, M. G.; Patrignani, P. De novo synthesis of cyclooxygenase-1 counteracts the suppression of platelet thromboxane biosynthesis by aspirin. *Circ. Res.* **2006**, *98*, 593−595.

(18) Grosser, T.; Smyth, E.; Fitzgerald, G. A. Anti-Inflammatory, Antipyretic, and Analgesic Agents: Pharmacotherapy of Gout. In *Goodman & Gilman's The Pharmacological Basis of Therapeutics*, 12th ed.; Brunton, L. L., Blumenthal, D. K., Murri, N., Dandan, R. H., Knollmann, B. C., Eds.; McGraw-Hill: New York, 2011; pp 962−992.

(19) Capone, M. L.; Tacconelli, S.; Sciulli, M. G.; Grana, M.; Ricciotti, E.; Minuz, P.; Di Gregorio, P.; Merciaro, G.; Patrono, C.; Patrignani, P. Clinical pharmacology of platelet, monocyte, and vascular cyclooxygenase inhibition by naproxen and low-dose aspirin in healthy subjects. *Circulation* **2004**, *109*, 1468−1471.

(20) García Rodríguez, L. A.; Tacconelli, S.; Patrignani, P. Role of dose potency in the prediction of risk of myocardial infarction associated with nonsteroidal anti-inflammatory drugs in the general population. *J. Am. Coll. Cardiol.* **2008**, *52*, 1628−1636.

(21) Capone, M. L.; Sciulli, M. G.; Tacconelli, S.; Grana, M.; Ricciotti, E.; Renda, G.; Di Gregorio, P.; Merciaro, G.; Patrignani, P. Pharmacodynamic interaction of naproxen with low-dose aspirin in healthy subjects. *J. Am. Coll. Cardiol.* **2005**, *45*, 1295−1301.

(22) Capone, M. L.; Tacconelli, S.; Sciulli, M. G.; Anzellotti, P.; Di Francesco, L.; Merciaro, G.; Di Gregorio, P.; Patrignani, P. Human pharmacology of naproxensodium. *J. Pharmacol. Exp. Ther.* **2007**, *322*, 453−460.

(23) Grosser, T.; Fries, S.; FitzGerald, G. A. Biological basis for the cardiovascular consequences of COX-2 inhibition: therapeutic challenges and opportunities. *J. Clin. Invest.* **2006**, *116*, 4−15.

(24) Massó González, E. L.; Patrignani, P.; Tacconelli, S.; García Rodríguez, L. A. Variability among nonsteroidal antiinflammatory drugs in risk of upper gastrointestinal bleeding. *Arthritis Rheum.* **2010**, *62*, 1592−1601.

(25) Tanaka, A.; Araki, H.; Komoike, Y.; Hase, S.; Takeuchi, K. Inhibition of both COX-1 and COX-2 is required for development of gastric damage in response to nonsteroidal anti-inflammatory drugs. *J. Physiol.* **2001**, *95*, 21−27.

(26) Patrono, C.; Patrignani, P.; García Rodríguez, L. A. Cyclooxygenase-selective inhibition of prostanoid formation: transducing biochemical selectivity into clinical read-outs. *J. Clin. Invest.* **2001**, *108*, 7−13.

(27) Dovizio, M.; Bruno, A.; Tacconelli, S.; Patrignani, P. Mode of action of aspirin as a chemopreventive agent. *Recent Results Cancer Res.* **2013**, *191*, 39−65.

(28) Rothwell, P. M.; Wilson, M.; Elwin, C. E.; Norrving, B.; Algra, A.; Warlow, C. P.; Meade, T. W. Long-term effect of aspirin on colorectal cancer incidence and mortality: 20-year follow-up of five randomised trials. *Lancet* **2010**, *376*, 1741−1750.

(29) Rothwell, P. M.; Fowkes, F. G.; Belch, J. F.; Ogawa, H.; Warlow, C. P.; Meade, T. W. Effect of daily aspirin on long-term risk of death due to cancer: analysis of individual patient data from randomised trials. *Lancet* **2011**, *377*, 31−41.

(30) Chulada, P. C.; Thompson, M. B.; Mahler, J. F.; Doyle, C. M.; Gaul, B. W.; Lee, C.; Tiano, H. F.; Morham, S. G.; Smithies, O.; Langenbach, R. Genetic disruption of Ptgs-1, as well as Ptgs-2, reduces intestinal tumorigenesis in Min mice. *Cancer Res.* **2000**, *60*, 4705−4758.

(31) Di Nunno, L.; Vitale, P.; Scilimati, A.; Tacconelli, S.; Patrignani, P. Novel synthesis of 3,4-diarylisoxazole analogues of valdecoxib: reversal COX-2 selectivity by sulfonamide group removal. *J. Med. Chem.* **2004**, *47*, 4881−4890.

(32) Perrone, M. G.; Vitale, P.; Malerba, P.; Altomare, A.; Rizzi, R.; Lavecchia, A.; Di Giovanni, C.; Novellino, E.; Scilimati, A. Diarylheterocycle core ring features effect in selective COX-1 inhibition. *ChemMedChem* **2012**, *7*, 629−641.

(33) Patrignani, P.; Panara, M. R.; Greco, A.; Fusco, O.; Natoli, C.; Iacobelli, S.; Cipollone, F.; Ganci, A.; Creminon, C.; Maclouf, J.; Patrono, C. Biochemical and pharmacological characterization of the cyclooxygenase activity of human blood prostaglandin endoperoxide synthases. *J. Pharmacol. Exp. Ther.* **1994**, *271*, 1705−1721.
(34) Patrono, C.; Ciabattoni, G.; Pinca, E.; Pugliese, F.; Castrucci, G.; De Salvo, A.; Satta, M. A.; Peskar, B. A. Low dose aspirin and inhibition of thromboxane B2 production in healthy subjects. *Thromb. Res.* **1980**, *17*, 317−327.
(35) Swinney, D. C.; Mak, A. Y.; Barnett, J.; Ramesha, C. S. Differential allosteric regulation of prostaglandin H synthase 1 and 2 by arachidonic acid. *J. Biol. Chem.* **1997**, *272*, 12393−12398.
(36) FitzGerald, G. A.; Pedersen, A. K.; Patrono, C. Analysis of prostacyclin and thromboxane biosynthesis in cardiovascular disease. *Circulation.* **1983**, *67*, 1174−1177.
(37) Tang, C.; Shou, M.; Mei, Q.; Rushmore, T. H.; Rodrigues, A. D. Major role of human liver microsomal cytochrome P450 2C9 (CYP2C9) in the oxidative metabolism of celecoxib, a novel cyclooxygenase-II inhibitor. *J. Pharmacol. Exp. Ther.* **2000**, *293*, 453−459.
(38) Zhang, J. Y.; Yuan, J. J.; Wang, Y. F.; Bible, R. H.; Breau, A. P. Pharmacokinetics and metabolism of a COX-2 inhibitor, valdecoxib, in mice. *Drug Metab. Dispos.* **2003**, *31*, 491−501.
(39) Tsai, A.; Kulmacz, R. Prostaglandin H synthase: resolved and unresolved mechanistic issues. *Arch. Biochem. Biophys.* **2010**, *493*, 103−124.
(40) Walker, M.; Kurumbail, R.; Kiefer, J.; Moreland, K.; Koboldt, C.; Isakson, P.; Seibert, K.; Gierse, J. A three-step kinetic mechanism for selective inhibition of cyclo-oxygenase-2 by diarylheterocyclic inhibitors. *Biochem. J.* **2001**, *357*, 709−718.
(41) Blobaum, A.; Marnett, L. Structural and functional basis of cyclooxygenase inhibition. *J. Med. Chem.* **2007**, *50*, 1425−1441.
(42) Ricciotti, E.; Dovizio, M.; Di Francesco, L.; Anzellotti, P.; Salvatore, T.; Di Francesco, A.; Sciulli, M. G.; Pistritto, G.; Monopoli, A.; Patrignani, P. NCX 4040, a nitric oxide-donating aspirin, exerts anti-inflammatory effects through inhibition of I kappa B-alpha degradation in human monocytes. *J. Immunol.* **2010**, *184*, 2140−2147.
(43) Cyrus, T.; Sung, S.; Zhao, L.; Funk, C. D.; Tang, S.; Praticò, D. Effect of low-dose aspirin on vascular inflammation, plaque stability, and atherogenesis in low-density lipoprotein receptor-deficient mice. *Circulation* **2002**, *106*, 1282−1287.
(44) Brater, D. C.; Harris, C.; Redfern, J. S.; Gertz, B. J. Renal effects of COX-2-selective inhibitors. *Am. J. Nephrol.* **2001**, *21*, 1−15.
(45) Ciabattoni, G.; Boss, A. H.; Patrignani, P.; Catella, F.; Simonetti, B. M.; Pierucci, A.; Pugliese, F.; Filabozzi, P.; Patrono, C. Effects of sulindac on renal and extrarenal eicosanoid synthesis. *Clin. Pharmacol. Ther.* **1987**, *41*, 380−383.
(46) Nasrallah, R.; Hébert, R. L. Prostacyclin signaling in the kidney: implications for health and disease. *Am. J. Physiol.: Renal Physiol.* **2005**, *289*, F235−F246.
(47) Rimon, G.; Sidhu, R. S.; Lauver, D. A.; Lee, J. Y.; Sharma, N. P.; Yuan, C.; Frieler, R. A.; Trievel, R. C.; Lucchesi, B. R.; Smith, W. L. Coxibs interfere with the action of aspirin by binding tightly to one monomer of cyclooxygenase-1. *Proc. Natl. Acad. Sci. U.S.A.* **2010**, *107*, 28−33.
(48) Jones, G.; Willett, P.; Glen, R. C.; Leach, A. R.; Taylor, R. Development and validation of a genetic algorithm for flexible docking. *J. Mol. Biol.* **1997**, *267*, 727−748.
(49) Bottegoni, G.; Cavalli, A.; Recanatini, M. A comparative study on the application of hierarchical-agglomerative clustering approaches to organize outputs of reiterated docking runs. *J. Chem. Inf. Model.* **2006**, *46*, 852−862.
(50) Kurumbail, R. G.; Stevens, A. M.; Gierse, J. K.; McDonald, J. J.; Stegeman, R. A.; Pak, J. Y.; Gildehaus, D.; Miyashiro, J. M.; Penning, T. D.; Seibert, K.; Isakson, P. C.; Stallings, W. C. Structural basis for selective inhibition of cyclooxygenase-2 by antiinflammatory agents. *Nature (London)* **1996**, *384*, 644−648.
(51) Thuresson, E. D.; Malkowski, M. G.; Lakkides, K. M.; Rieke, C. J.; Mulichak, A. M.; Ginell, S. L.; Garavito, R. M.; Smith, W. L. Mutational and X-ray crystallographic analysis of the interaction of dihomo-gamma-linolenic acid with prostaglandin endoperoxide H synthases. *J. Biol. Chem.* **2001**, *276*, 10358−10365.
(52) Gupta, K.; Selinsky, B. S.; Kaub, C. J.; Katz, A. K.; Loll, P. J. The 2.0 Å resolution crystal structure of prostaglandin H2 synthase-1: structural insights into an unusual peroxidase. *J. Mol. Biol.* **2004**, *335*, 503−518.
(53) Vecchio, A. J.; Simmons, D. M.; Malkowski, M. G. Structural basis of fatty acid substrate binding to cyclooxygenase-2. *J. Biol. Chem.* **2010**, *285*, 22152−22163.
(54) Luong, C.; Miler, A.; Barnett, J.; Chow, J.; Ramesha, C.; Browner, M. F. Flexibility of the NSAID binding site in the structure of human cyclooxygenase-2. *Nat. Struct. Biol.* **1996**, *3*, 927−933.
(55) Bhattacharyya, D. K.; Lecomte, M.; Rieke, C. J.; Garavito, M.; Smith, W. L. Involvement of arginine 120, glutamate 524, and tyrosine 355 in the binding of arachidonate and 2-phenylpropionic acid inhibitors to the cyclooxygenase active site of ovine prostaglandin endoperoxide H synthase-1. *J. Biol. Chem.* **1996**, *271*, 2179−2184.
(56) Yuan, C.; Rieke, C. J.; Rimon, G.; Wingerd, B. A.; Smith, W. L. Partnering between monomers of cyclooxygenase-2 homodimers. *Proc. Natl. Acad. Sci. U.S.A.* **2006**, *103*, 6142−6147.
(57) Yuan, C.; Sidhu, R. S.; Kuklev, D. V.; Kado, Y.; Wada, M.; Song, I.; Smith, W. L. Cyclooxygenase allosterism, fatty acid-mediated cross-talk between monomers of cyclooxygenase homodimers. *J. Biol. Chem.* **2009**, *284*, 10046−10055.
(58) Sidhu, R.; Lee, J.; Yuan, C.; Smith, W. Comparison of cyclooxygenase-1 crystal structures: cross-talk between monomers comprising cyclooxygenase-1 homodimers. *Biochemistry* **2010**, *49*, 7069−7079.
(59) Mbonye, U. R.; Yuan, C.; Harris, C. E.; Sidhu, R. S.; Song, I.; Arakawa, T.; Smith, W. L. Two distinct pathways for cyclooxygenase-2 protein degradation. *J. Biol. Chem.* **2008**, *283*, 8611−8623.
(60) Prusakiewicz, J. J.; Duggan, K. C.; Rouzer, C. A.; Marnett, L. J. Differential sensitivity and mechanism of inhibition of COX-2 oxygenation of arachidonic acid and 2-arachidonoylglycerol by ibuprofen and mefenamic acid. *Biochemistry* **2009**, *48*, 7353−7355.
(61) Zou, H.; Yuan, C.; Dong, L.; Sidhu, R. S.; Hong, Y. H.; Kuklev, D. V.; Smith, W. L. Human cyclooxygenase-1 activity and its responses to COX inhibitors are allosterically regulated by nonsubstrate fatty acids. *J. Lipid Res.* **2012**, *53*, 1336−1347.
(62) Dong, L.; Vecchio, A. J.; Sharma, N. P.; Jurban, B. J.; Malkowski, M. G.; Smith, W. L. Human cyclooxygenase-2 is a sequence homodimer that functions as a conformational heterodimer. *J. Biol. Chem.* **2011**, *286*, 19035−19046.
(63) Loll, P. J.; Picot, D.; Ekabo, O.; Garavito, R. M. The synthesis and use of iodinated non-steroidal antiinflammatory drug analogs as crystallographic probes of the prostaglandin H2 synthase cyclooxygenase active site. *Biochemistry* **1996**, *35*, 7330−7340.
(64) Lanzo, C. A.; Sutin, J.; Rowlinson, S.; Talley, J.; Marnett, L. J. Fluorescence quenching analysis of the association and dissociation of a diarylheterocycle to cyclooxygenase-1 and cyclooxygenase-2: dynamic basis of cyclooxygenase-2 selectivity. *Biochemistry* **2000**, *39*, 6228−6234.
(65) Suffert, J. Simple direct titration of organolithium reagents using *N*-pivaloyl-*o*-toluidine and/or *N*-pivaloyl-*o*-benzylaniline. *J. Org. Chem.* **1989**, *54*, 509−510.
(66) Di Nunno, L.; Scilimati, A. Synthesis of 3-aryl-4, 5-dihydro-5-hydroxy-1,2-oxazoles by reaction of substituted benzonitrile oxides with the enolate ion of acetaldehyde. *Tetrahedron* **1987**, *43*, 2181−2189.
(67) Di Nunno, L.; Scilimati, A.; Vitale, P. Regioselective synthesis and side-chain metallation and elaboration of 3-aryl-5-alkylisoxazoles. *Tetrahedron* **2002**, *58*, 2659−2665.
(68) Di Nunno, L.; Vitale, P.; Scilimati, A.; Simone, L.; Capitelli, F. Stereoselective dimerization of 3-arylisoxazoles to cage-shaped bis-*β*-lactams syn-2,6-diaryl-3,7-diazatricyclo[4.2.0.$0^{2,5}$]octan-4,8-diones induced by hindered lithium amides. *Tetrahedron* **2007**, *63*, 12388−12395.
(69) Di Nunno, L.; Scilimati, A.; Vitale, P. Reaction of 3-phenylisoxazole with alkyllithiums. *Tetrahedron* **2005**, *61*, 2623−2630.

(70) Di Nunno, L.; Scilimati, A.; Vitale, P. Effect of the aryl group substituent in the dimerization of 3-arylisoxazoles to *syn* 2,6-diaryl-3,7-diazatricyclo[4.2.0.0^{2,5}]octan-4,8-diones induced by LDA. *Tetrahedron* **2008**, *64*, 11198−11204.
(71) Di Nunno, L.; Scilimati, A.; Vitale, P. 5-Hydroxy-3-phenyl-5-vinyl-2-isoxazoline and 3-phenyl-5-vinylisoxazole: synthesis and reactivity. *Tetrahedron* **2005**, *61*, 11270−11278.
(72) Scilimati, A.; Vitale, P.; Di Nunno, L.; Patrignani, P.; Tacconelli, S.; Capone, M. L. Functionalized Diarylisoxazoles Inhibitors of Cyclooxygenase. U.S. Patent 7,989,450 B2, 2011.
(73) Pedersen, A. K.; FitzGerald, G. A. Cyclooxygenase inhibition, platelet function, and metabolite formation during chronic sulfinpyrazone dosing. *Clin. Pharmacol. Ther.* **1985**, *37*, 36−42.
(74) Ouellet, M.; Riendeau, D.; Percival, M. D. A high level of cyclooxygenase-2 inhibitor selectivity is associated with a reduced interference of platelet cyclooxygenase-1 inactivation by aspirin. *Proc. Natl. Acad. Sci. U.S.A.* **2001**, *98*, 14583−14588.
(75) Di Francesco, L.; Totani, L.; Dovizio, M.; Piccoli, A.; Di Francesco, A.; Salvatore, T.; Pandolfi, A.; Evangelista, V.; Dercho, R. A.; Seta, F.; Patrignani, P. Induction of prostacyclin by steady laminar shear stress suppresses tumor necrosis factor-alpha biosynthesis via heme oxygenase-1 in human endothelial cells. *Circ. Res.* **2009**, *104*, 506−513.
(76) Ciabattoni, G.; Pugliese, F.; Davi, G.; Pierucci, A.; Simonetti, B. M.; Patrono, C. Fractional conversion of thromboxane B2 to urinary 11-dehydrothromboxane B2 in man. *Biochim. Biophys. Acta* **1989**, *992*, 66−70.
(77) Pettersen, E. F.; Goddard, T. D.; Huang, C. C.; Couch, G. S.; Greenblatt, D. M.; Meng, E. C.; Ferrin, T. E. UCSF Chimera—a visualization system for exploratory research and analysis. *J. Comput. Chem.* **2004**, *25*, 1605−1612.
(78) DeLano, W. L. *The PyMOL Molecular Graphics System*; DeLano Scientific: San Carlos, CA, 2002.
(79) Lovell, S. C.; Word, J. M.; Richardson, J. S.; Richardson, D. C. The penultimate rotamer library. *Proteins* **2000**, *40*, 389−408.